Department of Mechanical Engineering

Equivalent shell element for passenger ship structural design

Eero Avi

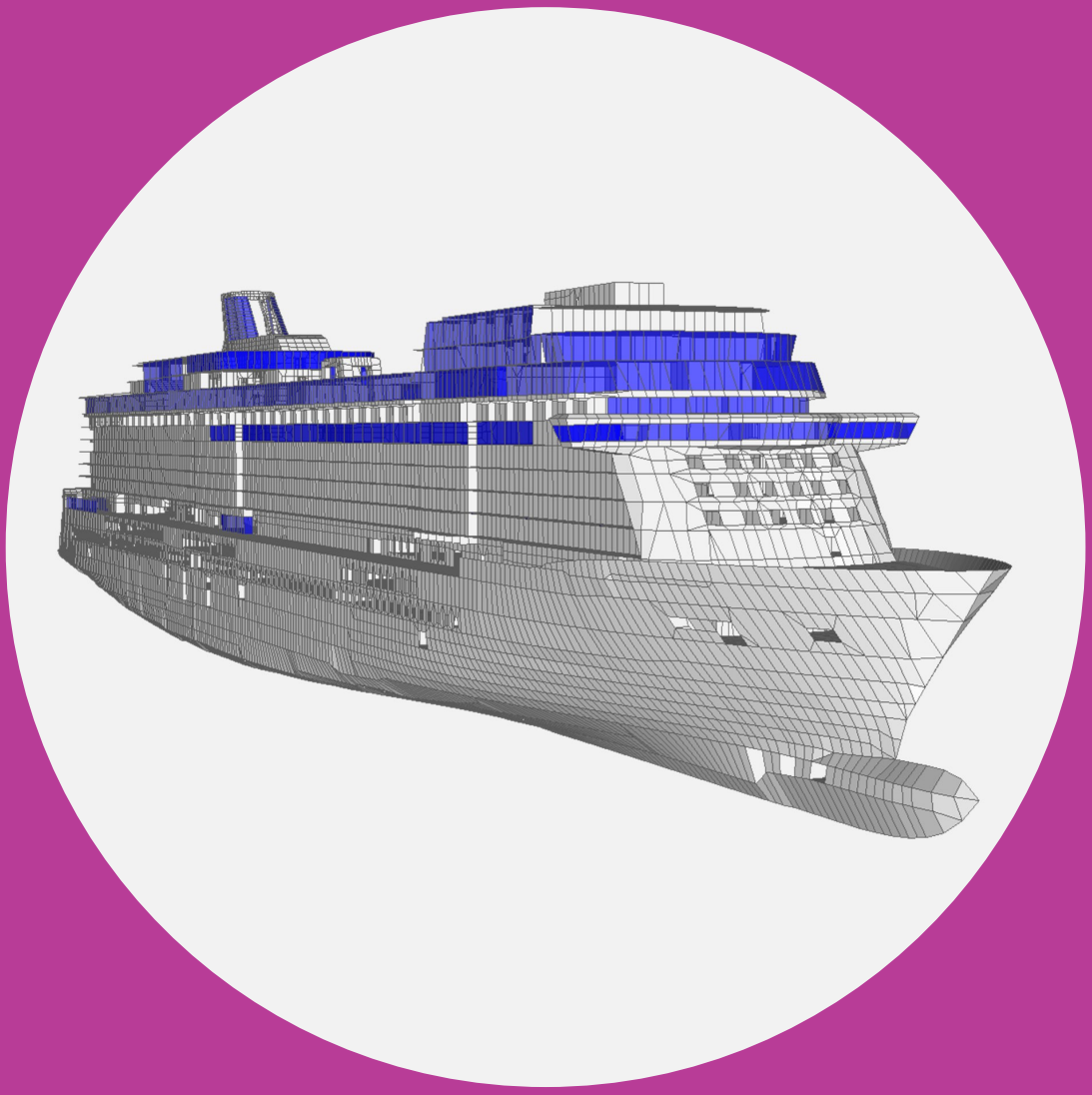

Aalto University

DOCTORAL DISSERTATIONS

Aalto University publication series
DOCTORAL DISSERTATIONS 133/2021

Equivalent shell element for passenger ship structural design

Eero Avi

A doctoral dissertation completed for the degree of Doctor of Science (Technology) to be defended, with the permission of the Aalto University School of Engineering, at a public examination held at remote connection link https://aalto.zoom.us/j/67023767762, and at the lecture hall K216 of the school on 22 October 2021 at 12 noon.

Aalto University
School of Engineering
Department of Mechanical Engineering
Marine Technology

Supervising professor
Professor Jani Romanoff, Aalto University, Finland

Thesis advisor
Professor Heikki Remes, Aalto University, Finland

Preliminary examiners
Professor Cesare Rizzo, University of Genova, Italy
Professor Jerolim Andric, University of Zagreb, Croatia

Opponents
Professor Cesare Rizzo, University of Genova, Italy
Lecturer Simon Benson, Newcastle University, United Kingdom

Aalto University publication series
DOCTORAL DISSERTATIONS 133/2021

ISBN 978-952-64-0531-5 (printed)
ISBN 978-952-64-0532-2 (pdf)
ISSN 1799-4934 (printed)
ISSN 1799-4942 (pdf)
http://urn.fi/URN:ISBN:978-952-64-0532-2

Unigrafia Oy
Helsinki 2021

Finland

Printed matter
4041-0619

Aalto University

Abstract

Aalto University, P.O. Box 11000, FI-00076 Aalto www.aalto.fi

Author
Eero Avi

Name of the doctoral dissertation
Equivalent shell element for passenger ship structural design

Publisher School of Engineering

Unit Department of Mechanical Engineering

Series Aalto University publication series DOCTORAL DISSERTATIONS 133/2021

Field of research Marine Technology

Manuscript submitted 9 April 2021 **Date of the defence** 22 October 2021

Permission for public defence granted (date) 26 August 2021 **Language** English

☐ **Monograph** ☒ **Article dissertation** ☐ **Essay dissertation**

Abstract

Predicting the global and local static and vibration response of a modern passenger ship is a challenging task, with major reliability and economic consequences if something goes wrong. Therefore, an accurate but computationally light calculation method is already needed in the early design phases when most of the important decisions are made. Currently, the ship's global response is investigated using a coarse mesh global Finite Element (FE) model, in which the mesh size equals the web-frame spacing. Girders are modelled with off-set beam elements and stiffeners together with plating using equivalent elements. Since the available equivalent elements do not or only partly consider the bending properties of the stiffened panel, the local response needs to be analysed separately using time-consuming sub-modelling technique. The objective of this thesis is to overcome the named limitations by introducing a more advanced equivalent element technique.

The stiffened panel can be considered as a three-layer laminate shell element, where the first layer represents the plate, the second layer the stiffener web and the third layer the stiffener flange. The element follows Equivalent Single Layer (ESL) First-order Shear Deformation Theory (FSDT). It includes membrane, membrane-bending, bending, and out-of-plane shear stiffness, the constitutive properties of which are found through a homogenisation process. This enables significant computational savings in design and further in the optimisation problem, as layer-wise formulation enables stiffened panel scantlings to be changed without remeshing the model, as well as accurate assessment of the stresses. However, for certain local engineering problems, this simplification is limited, since due to homogenisation process the local plate bending between the stiffeners is neglected. In static analysis the superposition principle can be used to fix the homogenised mean stress field with local oscillations resulting from the periodic structure. In vibration analysis, due to interaction of modes, more advanced correction is needed. For smaller panel-level problems, a single-degree-of-freedom spring-mass system-based solution is presented. For a larger structure, in which bulkheads, pillars, and girders are included, a kinetic and strain energy-based method is presented. The ranges of validity of the equivalent element with and without the additional local corrections have been defined and discussed. The case studies presented in this thesis focused on passenger ship structures, but the element can also be utilised for other ship types or large complex structures where fine mesh analysis is not justified.

Keywords equivalent element, equivalent single layer (ESL) theory, homogenisation, passenger ship, structural design, global finite element model, stiffened panel, static response, vibration response

ISBN (printed) 978-952-64-0531-5 **ISBN (pdf)** 978-952-64-0532-2

ISSN (printed) 1799-4934 **ISSN (pdf)** 1799-4942

Location of publisher Helsinki **Location of printing** Helsinki **Year** 2021

Pages 178 **urn** http://urn.fi/URN:ISBN:978-952-64-0532-2

Preface

The work presented in this thesis was carried out at the Marine Technology research group in the Department of Mechanical Engineering of Aalto University between 2014 and 2021. During the process I was funded by Aalto University School of Engineering, the Meyer Turku shipyard, LOURA (Lounaisrannikkoyhteistyö), and the FIMECC Sustainable Breakthrough Innovations project. The financial support is gratefully appreciated.

Research is teamwork, and I'm a very lucky guy to have had so many wonderful people around me during this journey. First, I would like to thank my supervisor, Prof. Jani Romanoff, and my thesis instructor, Prof. Heikki Remes, for their support and guidance during the entire process, but especially in the last year. I am very grateful for the time and effort they both invested in me. In addition, I would like to thank my wife Ingrit, who not only contributed to the content of thesis, but also provided valuable love, motivation, and support during all the ups and downs. I am also very grateful to Ari Niemelä, who gave me the opportunity in the first place to do my Master's thesis and then doctoral studies as a part-time student under the Meyer Turku shipyard. In addition, many thanks to Aleksi Laakso and Joni Raikunen for their contributions to the thesis.

I would also like to thank my other former colleagues from Meyer Turku: Risto Kuusjärvi, Heikki Lammi, Matti Rautiainen, Jussi Puurula, Ilkka Luotonen, Martin Kaldoja, and the rest of the Basic Hull department. During seven working years in the shipyard, I got nice memories and gained valuable industry experience, which helped me to build and write this thesis. I also appreciate my former and current colleagues from the Aalto University Marine Technology research group: Pauli Lehto, Sami Liinalampi†, Mihkel Kõrgesaar, Tanel Soa, Jasmin Jelovica, Sören Ehlers, Bruno Reinaldo Goncalves, Markus Ahola, Darko Frank, Mikko Suominen, Otto Puolakka, and many others for creating a positive, supportive, and motivating working atmosphere. I also wish

to thank Prof. Petri Varsta, who gave valuable feedback during postgraduate seminars and Prof. Pentti Kujala for his support, especially in the finalisation stage of the thesis. My gratitude also goes to the Aalto University support staff, who helped me in navigating through the paperwork, which is not always my strongest side.

I would especially like to thank the thesis pre-examiners, Prof. Cesare Mario Rizzo and Prof. Jerolim Andric, for their effort and valuable comments.

Finally, I would like to thank my family and friends and especially my little son, Kaur Robert, who taught me how to become more effective at work and showed how valuable quiet time for dedication can be.

Espoo, April 2021

Eero Avi

Contents

List of Publications

This doctoral dissertation consists of a summary and of the 5 following publications, which are referred to using following numerals:

[P1] Avi, Eero; Lillemäe, Ingrit; Romanoff, Jani; Niemelä, Ari. 2015. Equivalent shell element for ship structural design. Journal of Ship and Offshore Structures, volume 20, issue 3, pages 239-255. http://dx.doi.org/10.1080/17445302.2013.819689

[P2] Avi Eero; Laakso, Aleksi; Romanoff, Jani; Lillemäe, Ingrit. 2015. Simplified method for natural frequency analysis of stiffened panel, Analysis and Design of Marine Structures - Proceedings of the 5th International Conference on Marine Structures, MARSTRUCT 2015, pages pp.107-114. ISBN-13: 978-1138027893.

[P3] Laakso, Aleksi; Avi, Eero; Romanoff, Jani. 2019. Correction of local deformations in free vibration analysis of ship deck structures by equivalent single layer elements, Ship and Offshore Structures, volume 14, issue 1, pages 135-147. https://doi.org/10.1080/17445302.2018.1561173

[P4] Raikunen, Joni; Avi, Eero; Remes, Heikki; Romanoff, Jani; Lillemäe-Avi, Ingrit, Niemelä, Ari. 2019. Optimisation of passenger ship structures in concept design stage, Ship and Offshore Structures, volume 14, issue 1, pages 320-334. https://doi.org/10.1080/17445302.2019.1590947

[P5] Avi Eero; Laakso, Aleksi; Romanoff, Jani; Remes, Heikki; Lillemäe-Avi, Ingrit. 2021. Coarse mesh finite element model for cruise ship global and local vibration analysis, Marine Structures, volume 79, 103053. https://doi.org/10.1016/j.marstruc.2021.103053

Author's Contributions

Publication 1: Equivalent shell element for ship structural design.

The author developed an equivalent shell element technique for modelling stiffened panels in a ship global Finite Element model using the Equivalent Single Layer (ESL) plate theory. The author did all the FE analysis and wrote the manuscript. Lillemäe, Romanoff, and Niemelä contributed with valuable comments.

Publication 2: Simplified method for natural frequency analysis of stiffened panel.

The author extended Laakso's analytical method for combining global and local vibration modes for higher half-wave modes and for the ESL model. Originally, the method was limited to calculating only the first global half-wave mode. The author also carried out all the case studies and wrote the manuscript. Laakso, Romanoff, and Lillemäe contributed with valuable comments.

Publication 3: Correction of local deformations in free vibration analysis of ship deck structures by equivalent single layer elements.

Laakso developed a theory for modifying the generalised mass and stiffness of the ESL modes by considering the kinetic and strain energies of the local plate deformation. The research was outlined and the manuscript written together with the author. The author also assisted with the case studies and helped utilise the correction method for ESL theory-based models. Romanoff contributed with valuable comments.

Publication 4: Optimisation of passenger ship structures in concept design stage.

The work was initiated in Raikunen's Master's thesis, in which the author was an instructor. Raikunen created a MATLAB platform which linked the FE software and optimisation module together. The author helped to adjust the algorithm for an ESL theory-based model and prepared a prismatic cruise ship

FE model for the case studies. Together with Raikunen, the Author derived a solution for considering local strength effects in the optimisation process. Remes, Romanoff, Lillemäe-Avi and Niemelä made valuable comments on the manuscript.

Publication 5: Coarse mesh finite element model for cruise ship global and local vibration analysis

The author extended the correction method presented in [P3] for forced vibration analysis. He carried out the case studies and defined the validity boundaries of the ESL-theory based element in ship vibration analysis. Laakso and Romanoff contributed with constructive comments on the theory and outline of the paper. Remes and Lillemäe-Avi made valuable comments on the manuscript.

Original Features

In the design of modern passenger ships advanced strength and vibration assessment tools are already required in the early design phases. Utilising fine mesh Finite Element (FE) analysis on a global scale will lead to millions of degrees of freedom (DOF) and unreasonably high computational cost. Therefore, the hull girder-level response of the ship is today analysed using a coarse mesh FE model in which the element size normally equals that of the web frame spacing and only the membrane properties of stiffened panels are presented. Local structures are analysed separately using smaller fine mesh FE models. This leads to a significant number of sub-models and often some of the critical locations cannot be identified directly from such simple separated global or local FE models. This separation becomes even more problematic when analysis of the forced vibration induced by the propellers, main engines, and thrusters is performed. As the total vibration response is dependent on the frequency and mode shape, the couplings between the global and local model are difficult to define a priori.

The aim of this thesis is to increase the accuracy of a coarse mesh global FE model by developing an advanced equivalent shell element to represent the stiffened panels. This enables the local structural behaviour already to be predicted from a coarse mesh global FE model in the early design phases. The author believes that the following features of this thesis are original.

1. **Equivalent single layer (ESL) theory-based equivalent element modelling technique for representing stiffened panels [P1]**. The reference plane of the ESL element is defined in a way that allows geometrically exact coupling between the surrounding structures. Therefore, in addition to the membrane and bending, membrane-bending and out-of-plate shear stiffness are also considered. This leads to higher accuracy compared to existing commonly-used equivalent elements based on membrane or bending actions alone.

2. **The division of the stiffened panel into a three-layer laminate element [P1].** The element's first isotropic material layer represents the deck plate, and the second and third orthotropic material layers represent the stiffener web and flange, respectively. This layer-wise representation of ESL theory enables accurate homogenisation for both membrane and bending stiffness and stress estimations of each structural member separately. In addition, panel scantlings can be changed without remeshing the model.
3. **Utilising an ESL theory-based ship coarse mesh global FE model in hull girder optimisation [P4].** The laminate element's layer-wise formulation makes it convenient to be utilised for the optimisation of large complex structures. In addition, the lateral load cases can be directly applied to the global FE model, resulting in a more accurate combination of global and local responses. Since a higher discretisation level leads to increased hot-spot stresses, a constraint relaxation method is introduced in the optimisation process, i.e. a certain percentage of the area is allowed to violate the optimisation constraints. It is shown that by later strengthening those areas locally according to normal shipyard practice, it is possible to obtain significantly lighter designs.
4. **Correction methods for ESL theory-based element to consider plate vibration effects between the stiffeners were developed for a stiffened panel in [P2] and for the ship deck structure in [P3]. In [P5], the correction method was extended to forced vibration analysis.** None of the existing equivalent elements used for stiffened panels in a ship global FE model consider these local vibration effects. For stiffened panels only, a single-degree-of-freedom spring-mass system-based solution is developed. For more complex structures, a kinetic and strain energy-based method which can also be utilised in forced vibration analysis is presented.
5. **The boundaries of validity of an ESL theory-based equivalent element in the forced vibration analysis of a ship were extended and defined in [P5].** The ESL model is accurate in forced vibration analysis when the frequencies that are investigated are three times smaller than the local plate frequencies between the stiffeners, i.e. $\omega<\omega_{local}/3$. With the correction methods presented in [P3] and [P5], the limit can be extended to $\omega<\omega_{local}/1.5$.

List of Abbreviations and Symbols

Notations

A	membrane stiffness
A	cross section area
A_m	generalized amplitude of mode shape m
B	membrane bending stiffness
B, b	breadth
C_m	viscos damping for mode m
c_1	cognitive parameter
c_2	social parameter
D	bending stiffness
D_Q	out-of-plane shear stiffness
E	Young's modulus
el	element
F	force
G	shear modulus
h	height
I	inertia term
K	stiffness matrix
K_m	generalized stiffness of mode shape m
k	stiffness
L	length
M	mass matrix
M	moment
M_m	generalized mass of mode m
m	mass
m_d	deck plate mass between stiffeners
m_{da}	deck plate mass per area
N	normal force
n	node
P	pressure
p	the best location so far
Q	shear force
r_d	dynamic response of the midspan
S	stiffener spacing
s	local transverse coordinate between two stiffeners
T	transformation matrix
T_{Dzm}	deck plate z-directional part of kinetic energy
T_{LR}	local kinetic energy factor, which represents kinetic energy of unit deck area under unit amplitude

	enforced excitation of the global reference plane
T_{Cm}^{peak}	peak value of all translation kinetic energy of the model, except z-component of the deck plating
t	thickness
U_{LR}	strain energy of unit deck area under unit amplitude enforced excitation
U_{Cm}^{peak}	peak value of ESL model strain energy
u, v, w	displacements in x-, y- and z-directions
v	velocity vector of particle
w	inertia
X	response under forced vibration
x	current position vector of particle
α_n	effective element area which corresponds to a single node n

Greek symbol

γ	shear strain
ε	normal strain
θ	rotation of local plate between stiffeners
ν	Poisson's ratio
ρ	density
ς	critical damping
σ	normal stress
τ	shear stress
ϕ	vibration mode phase angle
φ	rotation
Ψ	mode shape deflection in z-direction
ω	angular frequency

General sub- and superscripts

avg	average
air	air between the stiffeners
b	bottom
cc	clamped-clamped boundary condition
cp	clamped-pinned boundary condition
ESL	ESL-theory based model
error	difference from fine mesh model results
f	flange
g	entire swarm
Gm	global mode shape of stiffened panel (without local plate vibration effects)
i	layer/particle
IM	imaginary part
k	iteration round
Lm	local mode shape of plate between the stiffeners

l	local	*RE*	real part
max	maximum	*s*	*stiffener*
m	vibration mode number	*t*	top
n	node number	*tot*	total
offs	offset	*w*	web
panel	Stiffened panel	0	reference plane location
p	deck plate		

Abbreviations

A-matrix model	FE model, where only membrane stiffness of stiffened panels is presented.
DOF	Degree of Freedom
ESL	Equivalent Single Layer
ESL model	FE model, where stiffened panels are modelled using ESL theory.
FSDT	First-order Shear Deformation Theory
FE	Finite Element
FEM	Finite Element Method
FEA	Finite Element Analysis
HP	Holland Profile
N.A	Neutral axis
PSO	Particle Swarm Algorithm
RHS	Rectangular Hollow Sections
RVE	Representative Volume Element
2D and 3D	Two and three dimensional

1 Introduction

1.1 Background

In the design of modern passenger ships, the goal is to improve onboard experience while reducing capital expenditure, i.e. CAPEX, and operating expenses, i.e. OPEX per passenger. To satisfy such conflicting requirements, several novel design concepts with new and challenging structural layouts and reduced scantlings have been investigated and larger vessels introduced. For example, the longitudinal strength of a cruise ship with a narrow superstructure was studied by Bergström in [1] and the concept has been applied in e.g. the MSC Seaside class and Virgin Voyages Scarlet Lady vessels. The feasibility of a 425.5-m mega-liner with a passenger capacity of 12000 was studied by Tsitsilonis et al. in [2]. The modularisation of the cabin area of a passenger ship, which leads to non-load-carrying accommodation decks, was analysed by Parmasto in [3]. Lillemäe et al. investigated the effect of using 3-mm thin superstructure decks and smaller HP profiles on hull girder response in [4]. Another recent trend in the industry is to reduce the scantlings of the primary T-girders to achieve lower mass and a smaller distance between superstructure decks, leading to a lowered centre of gravity and improved stability of the vessel; e.g. [5]. The lower centre of gravity can be utilised for extra features such as rollercoasters, water parks, or even kart tracks on the sun decks. Additionally, massive glass structures have been increasingly used in atriums, promenades, theatres, sun deck solariums, and elsewhere [6]. The outfitting of cruise ships now typically contributes more than 50% of the total mass of the superstructure, see Figure 1, but with the recent design solutions and passengers' expectations there is a tendency for it to increase even more [7]. To predict the global and local structural response of the hull of a large prototype vessel with an increased level of outfitting is very challenging. Insufficient structural analysis can lead to

over- or under-dimensioned design.[1] Additionally, it might be difficult to achieve a vibration comfort class [8] that matches the owner's expectations and contract, resulting in possible penalties for the shipyard and discomfort for the passengers and crew. To overcome the risk, accurate calculation methods need already to be involved in the early design phases, where major changes are possible and come at a low cost.

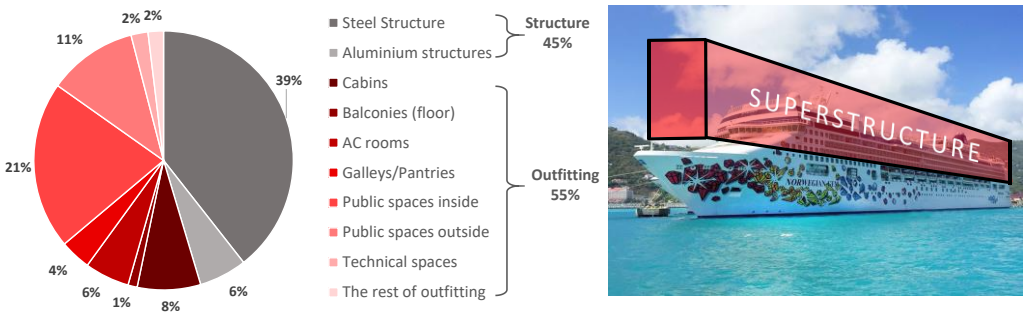

Figure 1: Cruise ship superstructure mass division [7]

Traditionally, the ship structural design of the ship can be divided into three stages: concept, basic, and detail design. Most of the important decisions are made in the concept design phase, such as defining the main characteristics of the ship, the preliminary general arrangement, and the main frame. During this stage, a general understanding of the behaviour and structural feasibility of the ship needs to be obtained to have enough input and confidence to proceed to the next stages. In the basic design, the concept of the ship is further developed, and the main scantlings are defined according to the structural analysis and classification society rules. Several iterations are necessary as the general arrangement of the ship evolves according to the design spiral [9]. At the end of the design process, classification drawings are made. After approval, detailed design starts, in which the design is finalised in terms of production and detail design requirements; see e.g. [10]. At the end of this stage, manufacturing drawings are available, and production can be prepared. In terms of man-hours this is the most time-consuming phase, as thousands of drawings need to be created. Therefore, only local changes are economically feasible, and all the necessary structural analysis must have been done beforehand.

According to the Ship Structural Committee (SSC) [11], the structural design of a cruise ship generally consists of two types of analysis: linear quasi-static

[1] Under-dimensioned design means that the ship structure does not meet the strength and/or vibration requirements. In over-dimensioned design, too-large structural scantlings are used. As a result, consequences resulting from increased weight such as higher cost, a lower outfitting level, decreased stability, and hydrodynamic performance, no longer justify the improved strength and vibration performance.

and vibration; see Figure 2. Complete analysis includes the response investigation at three different levels: primary, secondary, and tertiary [12]; see Figure 3. In the primary-level quasi-static response analysis, stresses and deformations of the hull girder resulting from hogging, sagging, racking, torsion, and docking load conditions are obtained [13]. Secondary response analysis focuses on the behaviour of a smaller structural unit under local loads, e.g. a deck structure under outfitting acceleration loads. The tertiary response level describes the behaviour of individual structural members, such as plates bending between stiffeners or stiffener warping. The responses in terms of stresses and deformations from these levels can be combined and compared against the serviceability and strength criteria set by the customer, authorities, classification societies, and the shipyard. The complete ship vibration analysis consists of three different types of analysis [14], [15]: 1) wave-induced hull girder, 2) propellers-, main engine- and thruster-induced, and 3) local machinery-induced vibration. Typically, wave-induced vibration analysis includes springing and whipping, for which accurate evaluation of the global natural frequencies of the hull girder is required [16], [17]. The propellers, main engines, and thrusters are usually the main source of such vibration that the passengers and crew will notice. In practical design, this kind of vibration is treated as a steady-state problem and solved in the frequency domain [16], [18]. Typical cruise ship first-order propeller frequencies are between 7 and 11 Hz and the ship engines are working in the range of 8-12 Hz. In addition to that, second-, third-, and higher-order frequencies also occur. The working frequency of bow and aft thrusters in a cruise vessel is approximately 11-15 Hz. This creates the most noticeable short-term vibration since the frequency is closest to the natural frequency of the deck structure. Sometimes separate local vibration analysis at a higher frequency (>15 Hz) needs to be performed as well, to investigate the response under higher-order propeller or main engine frequencies. There might also be some relevantly powerful machinery on board which can create noticeable local vibration. Depending on the vibration levels in various areas, ships can be graded into different comfort classes; see e.g. DNV-GL in [8] and Bureau Veritas (BV) in [14]. The exact class is predefined in the ship contract and usually for modern passenger vessels the highest comfort class is required. The class is validated on the basis of sea trial vibration measurements, which take place when the shipbuilding process is almost finalised and structural changes are no longer possible.

As stated by Keiramo in [19], the traditional structural design of passenger ship is moving towards the front-end of the design process as this is the stage

during which major architectural solutions are made, defining the success of the concept. The preliminary static and vibration analysis need to be performed already before the ship contract is signed. The evaluation methods must be computationally light but accurate enough to assess the structural response at a global and local level. The aim of this thesis is to present a method fulfilling these demands.

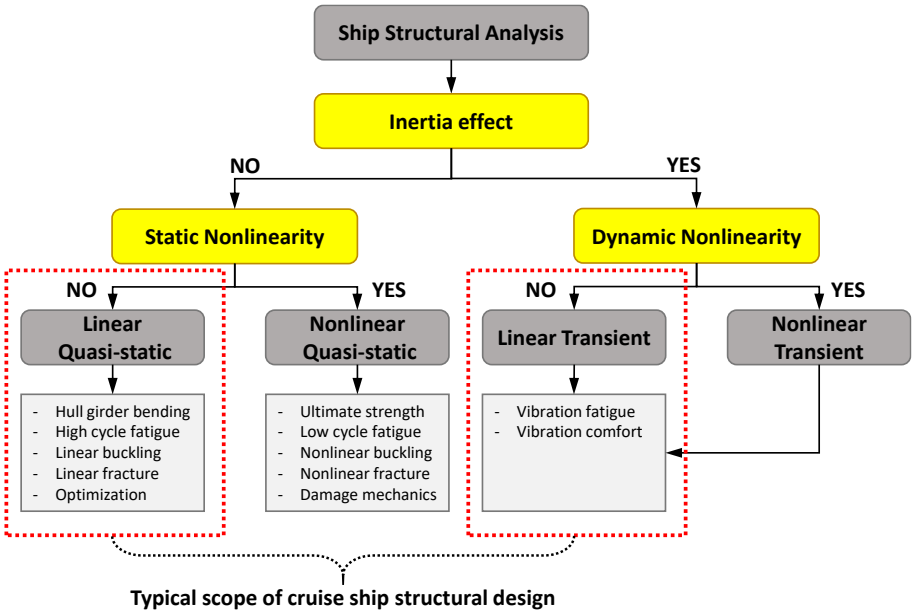

Figure 2: Ship analysis type flow chart and the typical scope of cruise ship structural design. Data is taken from [11].

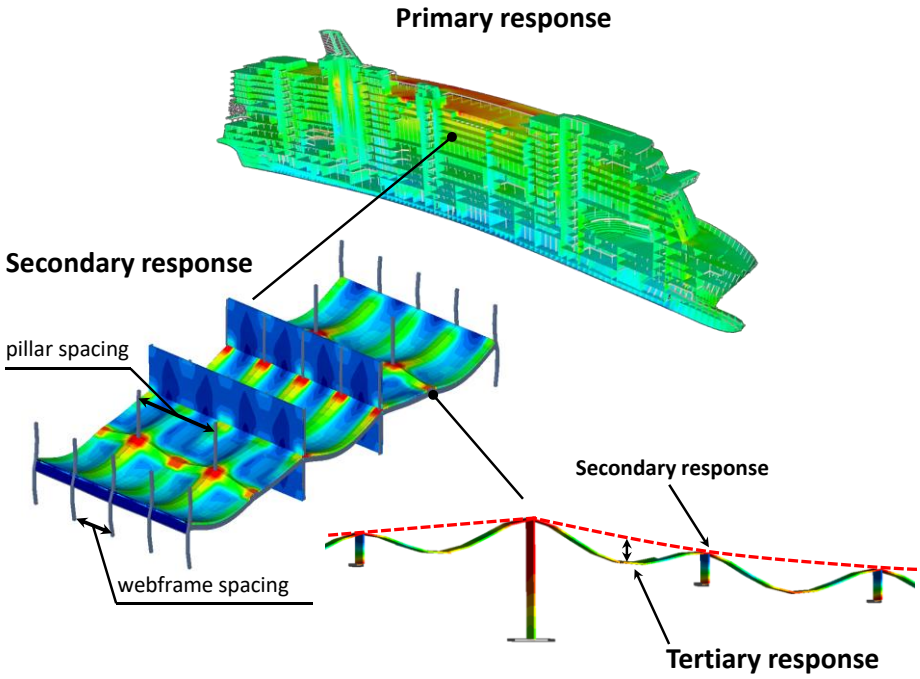

Figure 3: Global, i.e. primary, and local, i.e. secondary and tertiary response of the ship hull.

1.2 State of the Art

The basic approach for evaluating the global static bending response of a ship's hull girder is to use Euler-Bernoulli beam theory [20], [21], [22]. It is simple to use and for box-shaped vessels (tankers, barges, bulkers) it gives relatively accurate results [23], as the planes remain planes in bending, the deformed plane stays perpendicular to the mid-plane of the ship cross-section, and all structural members at the same location along the length bend the same amount. However, for cruise vessels, where hull-superstructure interaction occurs, these assumptions are violated and thus the theory is insufficient [24], [25]. Therefore, more advanced methods are needed. Crawford [26] was the first to develop a method based on two-beam theory, considering the longitudinal and vertical shear force caused by hull-superstructure interaction. Bleich [27] introduced a similar approach with vertical couplings, which allows a straightforward computation of stresses for prismatic ships. Terazava and Yagi proposed an approximate two-beam bending response calculation method which considers shear lag effects in [28]. In [29] the method was further developed to consider the effect of openings in the side-shell. Fransmann developed the analytical plane stress theory for multi-tier superstructures in [30]. Naar et al. [31] further developed Bleich's approach to a Coupled Beam (CB) theory, where the main idea is that the whole cross-section is divided into beams coupled to each other with springs. Because of its simplicity and low computational time, Naar's CB theory [31] has been applied in the structural optimisation process of ship hulls; see e.g. [5] [32], and [33].

Despite the significant development of the various analytical methods, finite element (FE) analysis is still regarded as the most reliable method for evaluating the structural behaviour of complex vessels such as cruise ships, yachts, container vessels, etc.; [11], [13], [34], [35]. The FE method offers several advantages. Geometrical discontinuities and hull shape can be well described and using a finer mesh enables the local response to be investigated with higher accuracy. FE analysis also allows the modelling of various load conditions and investigations of different materials and limit states including non-linear effects resulting from large displacements, material non-linear phenomena, and contact. For linear, static analysis, an overview with guidelines about creating a fine mesh global FE model of a ship is given in [36], where it is recommended to have a mesh size with at least two four-node shell elements between adjacent stiffeners when the local, i.e. tertiary bending response is to be assessed. A coarser mesh model could be used for analysis that is limited to the hull girder,

i.e. primary response, and when the membrane response is of interest. Large stiffeners and girders should be modelled using shell elements for web and beam elements for flanges and small stiffeners can be expressed as offset beam elements. As a result of this precise modelling, a lot of degrees of freedom (DOF) are introduced, which makes this method computationally extremely expensive, especially in the vibration analysis and optimisation process, where several design alternatives need to be modelled and analysed in a short time. The application for an optimisation problem can be simplified by using surrogate [37], [38] or sub-modelling techniques [39], but these methods are not applicable for complex vessels, where the sections are not identical and design changes significantly affect the global response. Therefore, fine mesh global FE models of ships are usually utilised for small vessels, where the number of DOF still remains reasonable, e.g. [40], [41], [42], [43], [44], but not for large cruise ships.

To reduce the modelling and calculation time, a full FE model of the cruise ship is created using a coarse mesh, in which only the main structural members are included; see Figure 4a. For concept design purposes, instead of a full FE model, a generic (prismatic) ship model can be used, the modelling principles of which are given in [45]. The standard mesh arrangement is normally one four- or eight-node quadrilateral element per web frame spacing and deck height. Ship door and window openings are modelled directly or using orthotropic plate element techniques, e.g. [46], [47], [48]. Because of their large participation in overall stiffness, the primary beams, i.e. web frames and girders, are explicitly modelled using offset beam elements. The ship's secondary stiffeners are incorporated into the plate or shell element formulation so that equivalent stiffness and mass are achieved. The most common way to represent a stiffened panel with an equivalent element is by lumping the stiffeners [23], [13]; see Figure 4c. In the lumping process, all secondary stiffeners are put inside the topological beam elements, which are located at the edges of the plate element. Each stiffener causes an increase in the cross-sectional properties of the lumped beam element. With this approach, the membrane stiffness of the stiffened panel is presented, but bending properties are neglected. In practice, this modelling technique has a major shortcoming. In addition to the stiffener type, the beam element properties are also dependent on the mesh size, which results in significant extra hours in the modelling and post-processing stages. To overcome this issue, this type of equivalent element can be modelled using a two-layer plate element, in which the first layer represents the deck plating and the second layer the stiffeners,

which are smeared evenly along the plating; see Figure 4d. The stiffener layer is described using 2D orthotropic material, which has axial stiffness in only one direction; see Hughes [23]. The stiffness matrix of the complete stiffened panel is obtained by summing the stiffness matrices of the plate and the "stiffener element". Davies developed a rectangular plane stress element to represent the stiffened panel in [49], where the element stiffness matrix is expressed by analytic formulae. The panel bending stiffness is neglected, but the bending stresses were evaluated using common analytical formulae. The element was used in the optimisation of a ship structure in [50] and together with [23] is available in the MAESTRO and OCTOPUS structural design software [45].

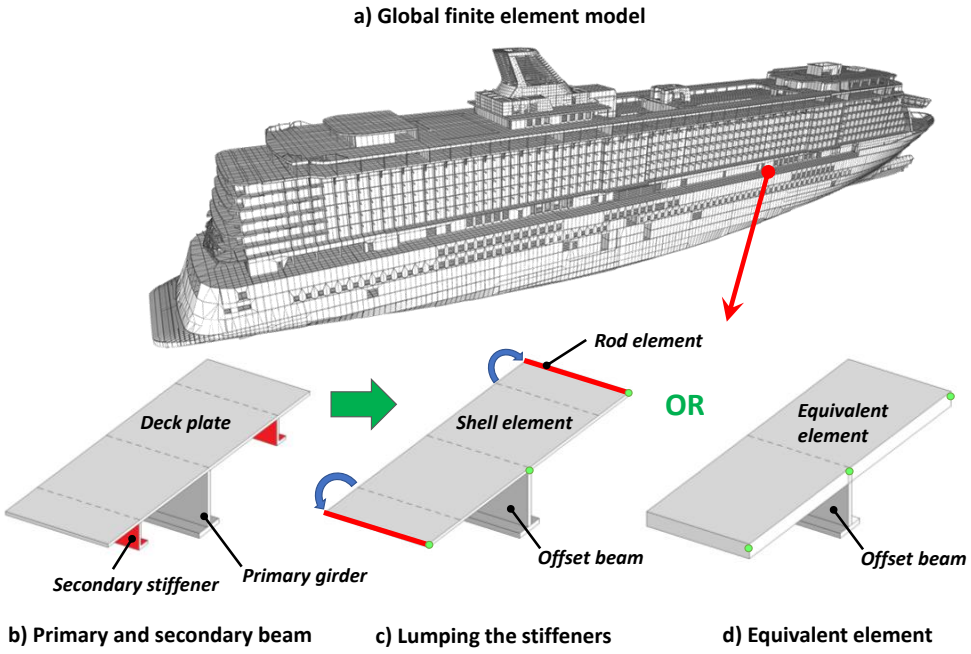

Figure 4: Global FE model (a), main structural components (b), and their modelling options (c, d).

The above-mentioned equivalent element techniques represent only the membrane stiffness of the stiffened panel. This simplification is possible as ship hull girders are thin-walled structures which carry the global deformations mainly in membrane action. For secondary and tertiary response analysis, local areas need to be analysed separately with a 3D fine mesh. For that the sub-modelling technique, in which the global problem is transformed into a smaller interface problem, can be used. The displacements, forces, or stresses at the boundaries of the local area of interest are obtained from the coarse mesh global model and are applied to the relevant nodes of the refined local model; see Figure 5. The Domain Decomposition Method (DDM) was applied in static analysis of a passenger ship in e.g. [51]. For a large cruise vessel, a high number of sub-models is needed and not all critical locations can be identified from the

coarse mesh FE model. Thus, the method is computationally expensive. DDM is also difficult to apply for forced vibration analysis, as different modes interact and thus it is very challenging to make couplings between the global and local FE models.

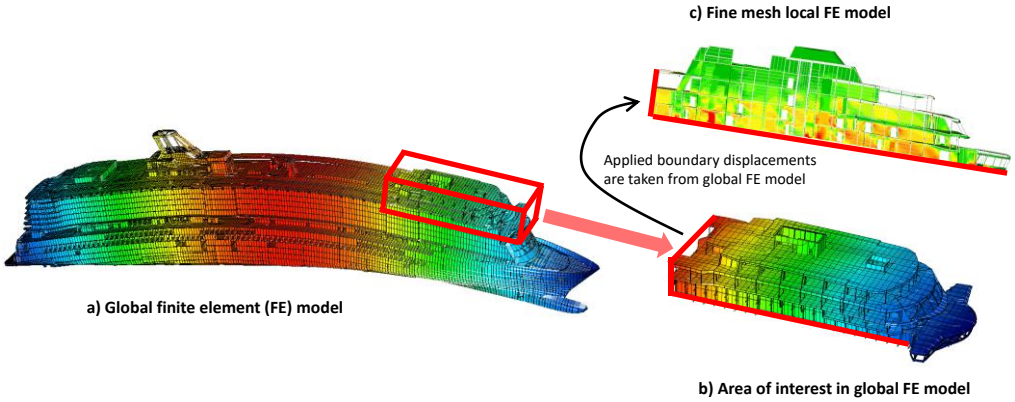

Figure 5: The principle of the sub-modelling technique.

To perform local structural analysis directly in a coarse mesh global FE model, the bending properties of the stiffened panel need to be included. Hughes [23], Paik [52], and Benson et al. [53] developed the orthotropic plate approach further by including the bending and torsional rigidity of the stiffeners. The stiffness properties are derived using the governing non-linear differential equations of large deflection orthotropic flat plate theory. Thus, the methods can be used to evaluate the ultimate strength of stiffened panels. While the stiffness properties remain constant in [52], they are recalculated at each increment of end displacement in [53]. In addition to that, stiffened panels can be represented by combining the Allman's plane stress element [54] with the discrete triangular plate-bending element [55]; for more details see [56]. However, both methods have several shortcomings. The bending properties are included but coupling between stiffened panel bending and membrane actions is missing. In the orthotropic plate approach out-of-plane shear stiffness properties are also neglected. Since the stiffeners are smeared into the plating, the stresses in the stiffener web and flange separately cannot be directly extracted. Additionally, triangular elements used in [56] are less accurate for performing local response analysis compared to rectangular shape elements [36].

The theory of the orthotopic elements that are discussed – [52], [53] – principally follows the features of a homogenisation process, in which the periodic structure is analysed using a computationally light macro-scale model, the constitutive properties of which are obtained from the microscale problem.

Homogenisation is a broadly used technique for creating calculation models of heterogenous composite structures, the structural complexity of which could be even higher than in a stiffened panel. There are various theories available - see e.g. [57]-[61] - but fundamentally they follow the same idea. The 3D periodic panel structure is represented by a homogenised shell continuum in which the stress or strain distribution through the thickness needs to be similar to that in a real structure. In a simple case, Kirchhoff-Love plate theory can be used, but for more advanced problems Equivalent Single Layer First-order Shear Deformation Theory (ESL-FSDT) [62] or even Zig-Zag multilayer plate theories [63] can be applied. The constitutive stiffness properties of such a macroscale model are obtained from the microscale model, which represents the unit cell of a repeatable structure. As this represents the volume of the corresponding local macro element, it is commonly named the Representative Volume Element (RVE). It is assumed that the RVE is infinitely small compared to a macroscale model and local tertiary effects have a minor influence on the overall behaviour of the actual panel. As the stress or strain distribution is assumed to be similar in both models, the macroscale model can be used to formulate the boundary conditions for finding the average stiffness properties of the RVE model, which can then be analysed through numerical or analytical methods. As a result, even a complex periodic structure can be simplified into a shell element formulation.

Because of their benefits, homogenisation theories have also been applied in the response analysis of ship sandwich panels. Buannic et al. presented the Kirchhoff-Love homogenised plate approach for various sandwich panels in [64]. The homogenised constitutive properties were found from a unit cell model using the analytical expressions presented in [65]. The theory is suitable for a symmetric structure, in which the reference plane corresponds to the geometrical midplane. Thus, the panel membrane [A] and bending [D] stiffness properties are considered, but membrane-bending coupling [B] is neglected. Case studies revealed that under bending the out-of-plane shear effects could be significant and therefore for a macroscale model the Reissner-Mindlin homogenised shell element should be preferred. To overcome these limitations, Romanoff and Varsta developed a theory for asymmetric sandwich panels in [66]. The macroscale homogenised model follows ESL-FSDT [62], but in addition it also has a stabilising layer accounting for the finite bending stiffness of the face plates, which has a significant effect on the local curvature of the panels under shear loads. When this effect is set to be very small, the internal forces, strain, and curvature can be represented according to the FSDT [62]. The constitutive equations were obtained analytically by dividing the unit cell model

into three separate layers, in which the face plates follow the isotropic Kirchhoff-Love plate theory. The core elasticity matrix was obtained by applying the Rule of Mixtures together with Voigt [67] and Reuss [68] approximation. As such a macro element presentation enables high accuracy with low computational cost, it has been utilised in several sandwich structure optimisation works, such as a hoistable car deck [69] or superstructure deck [70]. The theory was applied to an equivalent stiffness matrix shell element in which homogenised stiffness matrix components, i.e. [A], [B], [D] and out-of-plane shear stiffness [D_Q], were derived with respect to a reference plane, which was chosen to be at the geometrical mid-plane. However, in principle the selection of the reference plane is free and it can be selected anywhere over the thickness [71]. As shown by Reinaldo Goncalves et al. [72], this is important in post-buckling problems as the buckling of one face causes bending membrane coupling in panels even if the reference plane is selected to be equal to the "neutral axis" in the strong direction. In [73] this interaction was considered using an offset transformation matrix, which adjusted the beam element stiffness matrix accordingly. However, for large ship structures this tedious solution is not practical as there are too many stiffened panel/T-girder combinations to be created and the continuity of the structures must be ensured in the modelling.[2] Additionally, a limitation occurs in vibration analysis. As the homogenised stiffness properties are used, the deck plate behaviour between the stiffeners cannot be represented and the size of the stiffener spacing with respect to the characteristic length of the deformation needs to be revisited. These effects will cause the highest error in modes where the natural frequencies of the stiffened panel and the plate between the stiffeners interfere with each other. In a linear static response, this interaction could be considered using simple superposition principle [66] but for vibration analysis, a more advanced solution needs to be developed. Neglecting tertiary bending effects also causes limitations in non-linear analysis, where the global elastic buckling of panels can be captured with good accuracy, but when local face plate buckling modes between the webs start to occur, the accuracy will drop significantly; see [74], [75], [76]. To overcome this problem, the sandwich panel homogenisation theory was later extended to micropolar plates and different core geometries by Karttunen et al [77] and Nampally et al. [78] in a micropolar setting, which is based on non-classical continuum mechanics. However, these theories are currently limited to the

[2] In a stiffened panel the only continuous layer with a load-carrying capability in the *x*-, *y*-, and *xy*-directions is the plate layer, which never coincides with the "neutral axis" concept derived from the beam theory.

panel level only and are difficult to apply in the response analysis of larger ship structures using commercial software.

1.3 Objectives and Scope

The aim of this doctoral thesis is to develop an equivalent element technique for representing stiffened panels to assess the global and local static and vibration response of a ship with high accuracy and low computational cost. This would also bring significant benefits for the industry since more information can already be directly obtained from the global FE model in the early design phases. As a result, challenging concepts can be implemented with lower risk and cost.

The research is composed of five papers; see Figure 6 . The aim of the first paper [P1] is to extend the homogenisation theory of sandwich panels for stiffened panels presented in [66] and to develop a practical modelling technique which considers the interaction between primary girders and the equivalent element in a more convenient way. In the homogenised macro model the bending properties between stiffeners are neglected. As shown in [66] for static analysis, it could be considered using a simple super-positioning principle. However, because of the vibration analysis inertia effects and mode interaction, the problem seems more complex, and another solution needs to be developed. In the second paper [P2] such tertiary vibration effects are studied and a correction method for the stiffened panel level is developed. In the third paper [P3], the correction method is further developed so that it can be utilised for typical ship deck structures, including T-girders, bulkheads, and pillars. The aim of the fourth paper [P4] is to utilise the ESL theory-based element in a cruise ship optimisation problem. In the fifth paper [P5], the correction method developed in [P3] is extended to forced vibration analysis and the range of the element's validity in the structural design of cruise ships is comprehensively defined.

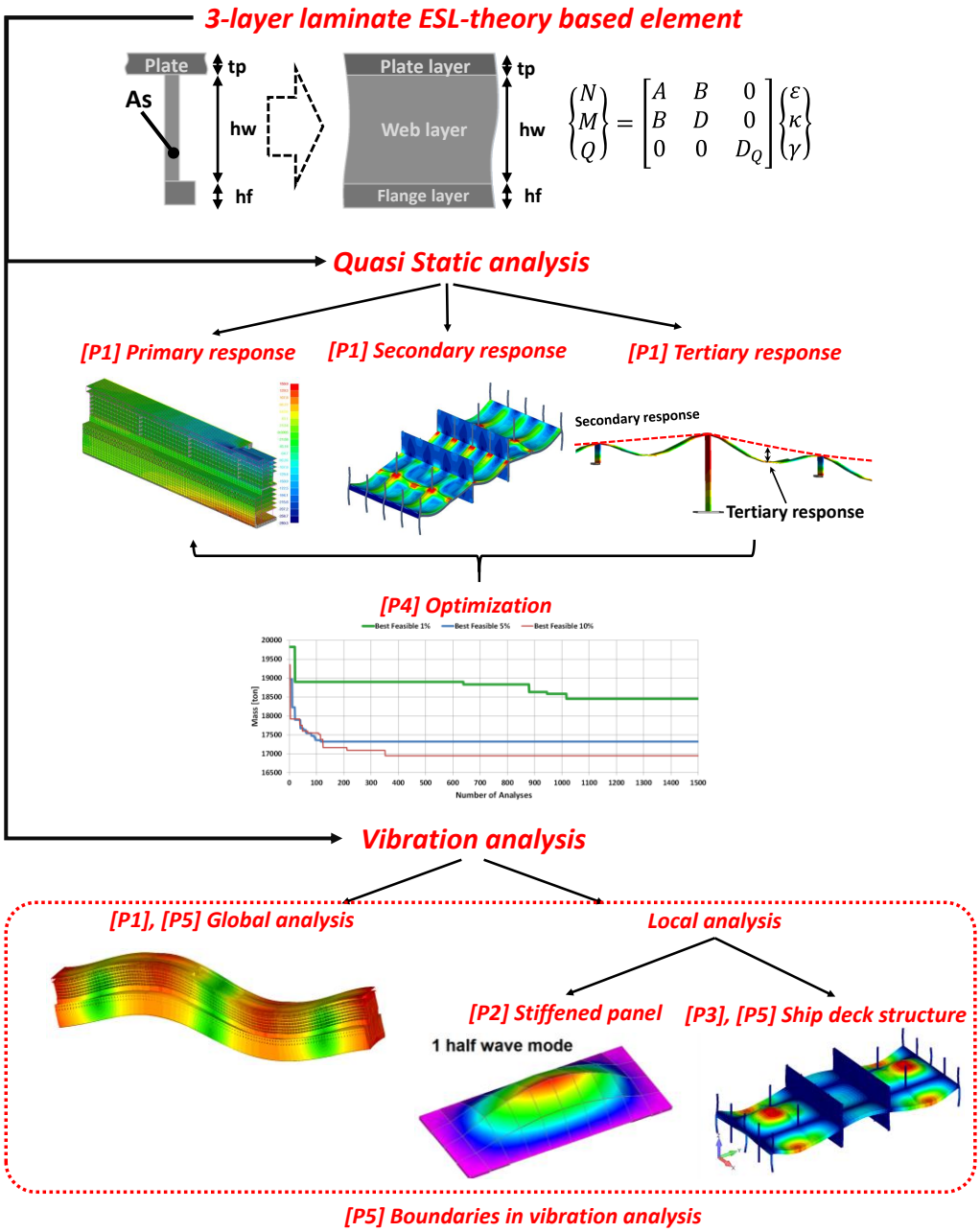

Figure 6: Framework of the thesis.

1.4 Limitations

The research is limited to flat stiffened panels where the stiffeners are parallel to each other and are located perpendicular to the attached plate. In practical design this limitation is very common and in a global FE model such curved areas as the hull shape are expressed by using several flat quadrilateral or triangular elements, e.g. [13], [18], [79], [80]. In addition, to represent the stiffened panel, the cross-section of the HP-profile is idealised as a rectangular L-profile, the dimensions of which result in an equal mass and second moment of area as in the original profile. For primary beams, the stiffener and outfitting

cut-outs are excluded. Additionally, the minor structural members, such as brackets, collar plates, scallops, etc., are excluded in equivalent element and fine mesh FE models.

The presented element that is presented is limited to quasi-static linear-elastic and steady-state harmonic vibration analysis. In cases where hull girder vibration is studied, only dry modes are considered in order to avoid any additional disturbance in the results from added water effects. In addition, the effect of residual stresses and preload effects are neglected. Furthermore, the effect of outfitting (window glasses, levelling concrete, floor tiles, etc.) on the structural stiffness is neglected.

The correction methods developed for local static and vibration analysis assume that locally only a clamped-clamped first half-wave mode between the stiffeners occurs. Global flexural waves are assumed to be long in comparison to the stiffener spacing. The tertiary effects of the secondary stiffeners, i.e. warping and tripping, are neglected, as they become more relevant in higher-frequency vibration analysis and in limit state condition [23].

In optimisation, the loading that is applied is calculated only at the beginning of the optimisation process and remains constant. The effect of changes in structural mass and its distribution is assumed to be small compared to the total hull girder bending moment. As the focus of the thesis is on utilising and testing the equivalent element technique develop here in a ship hull girder optimisation problem, the algorithm has only one objective, i.e. lower mass. Additional objective functions can be added and, for example, production cost can be evaluated by using methods described in [81] and [82].

2 Finite element model

2.1 Equivalent element for stiffened panels

According to [P1], ships' stiffened panels can be regarded as periodic structures, in which a repeatable unit (unit cell) contains one stiffener together with the deck plating. The width of the unit equals the stiffener spacing, the height is the plate thickness plus the stiffener height and the length is some arbitrary length along the direction of the stiffener (infinitesimal, or characteristic length of deformation). As a result of this assumption, the 3D panel geometry can be modelled as a computationally light layer-wise shell continuum, which follows Equivalent Single Layer First-order Shear Deformation Theory (ESL-FSDT). The element includes the membrane [A], membrane-bending coupling [B], bending [D], and out-of-plane shear stiffness [D_Q], the homogenised constitutive properties of which are obtained analytically from the stiffened panel unit cell, i.e. the RVE model. The homogenisation process is shown in Figure 7.

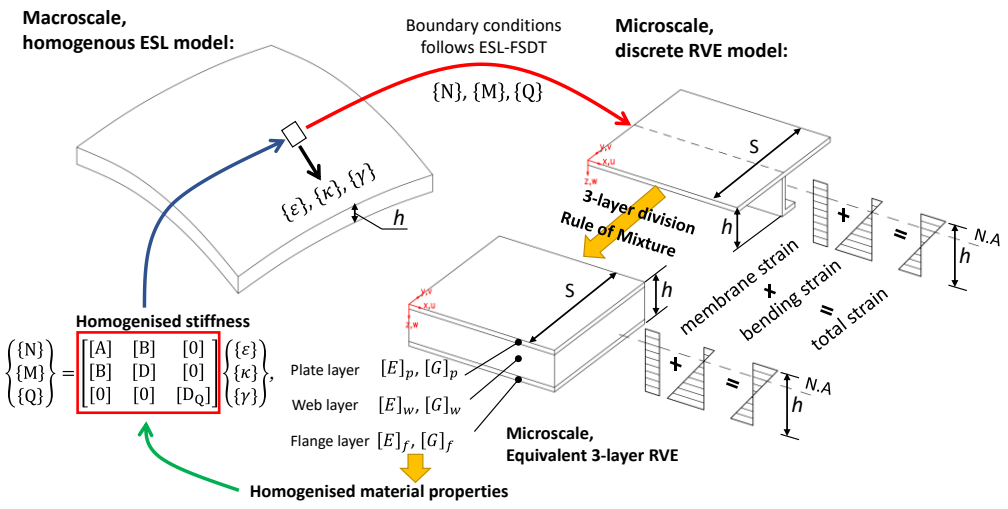

Figure 7. Homogenisation process of equivalent element for stiffened panel.

The stiffened plate is divided into three layers, where the plate layer thickness t_p equals that of the deck plate and, the web and flange layer thicknesses h_w and h_f correspond to the height of the stiffener web and flange, respectively; see

Figure 8. Thus, the total height equals the height of the stiffened panel that is being represented. The element reference plane is located on the bottom of the deck plate. Because of this layer-wise division deriving constitutive equations for the 3D panel geometry becomes relatively easy. The deck plate layer is described by isotropic material model and the stiffener layers by orthotropic ones, in which the homogenised material properties are found from the Rule of Mixtures. The micro-to-macro-scale transition is established by the Hill-Mandel condition [83], where it is assumed that the average work done in RVE equals to the corresponding local work in the macroscale model. The boundary conditions of the RVE problem are formulated on the basis of the membrane deformation and the curvature of the ESL theory-based macroscale model. Thus, it is assumed that in both models the strain through the thickness is linearly distributed. and stiffener warping can be neglected.

Another simplification is made by excluding the local plate bending moments between the stiffeners. This can be achieved by assuming that the plate fields between the webs undergo cylindrical bending as a result of local uniform pressure. For this deformation shape, the volume average of the bending moments is zero. In addition, the local inertia terms are left out by assuming that the stiffener spacing is infinitely small in relation to the characteristic length of the panel deformation, i.e. S/B or $S/L \rightarrow 0$. The assumption is valid in classical continuum mechanics formulations, where the material point associated with RVE is assumed to be infinitesimal in the macroscale structural model, i.e. in the FSDT shell. Although neglecting the local plate bending between stiffeners is a justified simplification for most of the structural analysis of ships, for some local engineering problems the ESL theory-based element that is utilised is limited, and local effects need to be recoupled. For more details, see Chapter 3 and Chapter 4.

With the simplification applied the equivalent element becomes computationally very light and easy to apply in large-scale models. The theory, together with its application, is supported by the most common FE software, e.g. Nastran, ANSYS, and ABAQUS, where a laminate shell element can be used, which follows ESL-FDT. To represent the stiffness couplings between the stiffened panel and T-girder correctly, the reference plane of the laminate element should be offset from the geometrical mid-plane to the interface of the deck plate and stiffener web as shown in Figure 8. This also ensures proper transfer of loads and responses between the primary, secondary, and tertiary levels. Moreover, in vibration it is crucial that the mass distribution between

structural members is described in a realistic way. In a cruise vessel, most of the significant outfitting mass is located on top of the decks. This means that the centre of gravity of the stiffened panel, together with the outfitting mass, is closer to the plate surface than to the geometrical mid-plane.

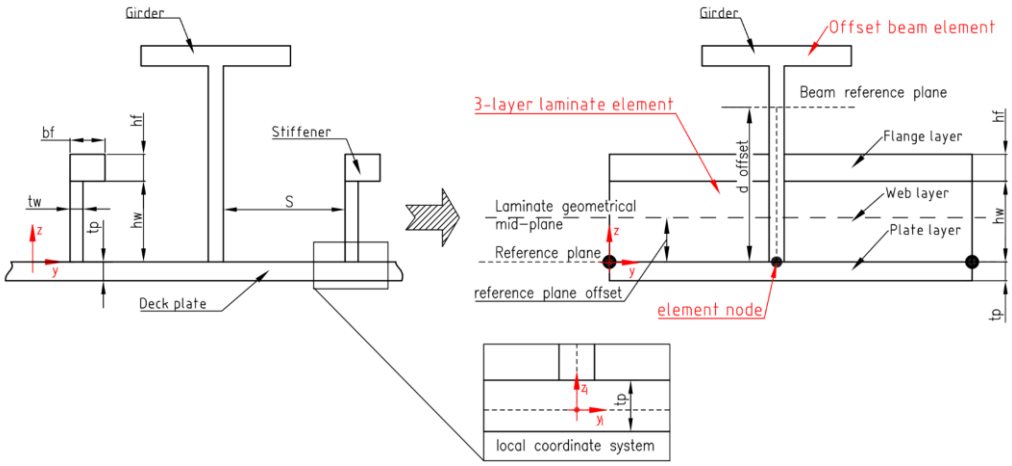

Figure 8. Division of a stiffened panel into a three-layer laminate element [P4].

2.1.1 Kinematics

The x-direction of the stiffened panel is taken parallel to the stiffener orientation, while the z-direction is normal to the plane; see Figure 8. The x, y, and z displacements are denoted by u, v, and w, respectively, and can be divided into two parts, namely the global and the local plate deflection. Thus, the displacements are given as:

$$u(x,y,x_l,y_l,z,z_l,p) = u_0(x,y,p) + z\varphi_x(x,y,p) + z_l\theta_{x,l}(x,y,x_l,y_l,p),$$

$$v(x,y,x_l,y_l,z,z_l,p) = v_0(x,y,p) + z\varphi_y(x,y,p) + z_l\theta_{y,l}(x,y,x_l,y_l,p),$$

$$w(x,y,x_l,y_l,z,z_l,p) = w_0(x,y,p) + w_{0,l}(x,y,x_l,y_l,p), \qquad (1)$$

where the subscript o denotes the displacements at the reference plane and z is the distance from the reference plane of the stiffened panel and z_l from the mid-plane of the deck plate in question. The rotations are taken as:

$$\varphi_x = \gamma_{xz} - \frac{\partial w_0}{\partial x} = \frac{\partial u}{\partial z},$$

$$\varphi_y = \gamma_{yz} - \frac{\partial w_0}{\partial y} = \frac{\partial v}{\partial z}, \qquad (2)$$

$$\theta_{x,l} = -\frac{\partial w_{0,l}}{\partial x_l},$$

$$\theta_{y,l} = -\frac{\partial w_{0,l}}{\partial y_l}.$$

The stiffened panel follows FSDT, but the deck plate bends as a Kirchhoff plate between the stiffeners. Assuming that the transition between local and global behaviour can be separated, the strains are:

$$\varepsilon_{xx} = \frac{\partial u}{\partial x} + z\frac{\partial \varphi_x}{\partial x} + z_l\frac{\partial \theta_{x,l}}{\partial x_l},$$

$$\varepsilon_{yy} = \frac{\partial v}{\partial y} + z\frac{\partial \varphi_y}{\partial y} + z_l\frac{\partial \theta_{y,l}}{\partial y_l},$$

$$\gamma_{xy} = \frac{\partial u_0}{\partial y} + \frac{\partial v_0}{\partial x} + z\left(\frac{\partial \varphi_y}{\partial x} + \frac{\partial \varphi_x}{\partial y}\right) + z_l\left(2\frac{\partial \theta_{y,l}}{\partial x_l \partial y_l}\right), \quad (3)$$

$$\gamma_{xz} = \frac{\partial w_0}{\partial x} + \varphi_x,$$

$$\gamma_{yz} = \frac{\partial w_0}{\partial y} + \varphi_y.$$

2.1.2 Constitutive equations

According to the three-layer division - see Figure 8 - the first layer, i.e. the deck plate layer elasticity matrix $[E]_p$, can be described using 2D isotropic material:

$$[E]_p = \frac{E}{1-\nu^2}\begin{bmatrix} 1 & \nu & 0 \\ \nu & 1 & 0 \\ 0 & 0 & \frac{(1-\nu)}{2} \end{bmatrix}. \quad (4)$$

The second and third layers, i.e. the web and flange layers, should have different stiffness in the x and y-directions. Thus, a 2D orthotropic material model is used. These layers can be regarded as composite material, in which the fibre represents the stiffeners and the matrix is the air between them. To find the homogenised properties of such a combination, the Rule of Mixtures is used, which can be described by two material models: Reuss uniform stress approximation [68] (lower bound stiffness) or Voigt strain approximation (upper bound stiffness) [67]. The first model assumes that under loading the stress remains the same in the composite, fibre, and matrix, i.e. $\sigma_{eq} = \sigma_s = \sigma_{air}$, while in the second model the strains are equal, i.e. $\varepsilon_{eq} = \varepsilon_s = \varepsilon_{air}$. The strain-based homogenisation is normally applied to calculate the elastic modulus in the fibre direction, while the stress-based is used for estimations in the transverse direction [84]. On the basis of those relationships the average Young's modulus for the stiffener direction E_x^{avg} and opposite to the stiffener direction E_y^{avg} are obtained:

$$E_x^{avg} = E_s\frac{A_s}{A_{tot}} + E_{air}\frac{A_{air}}{A_{tot}}, \quad (5)$$

$$E_y^{avg} = \frac{A_{tot}(E_s E_{air})}{(A_s E_{air})+(A_{air} E_s)}, \quad (6)$$

where the subscripts *s* and *air* donate the stiffener and air, respectively, and A_{tot} represents the layer cross-section area of RVE, i.e.the layer height multiplied by the stiffener spacing *S*. As the air stiffness can be regarded as zero, the stiffener layers have stiffness only in the longitudinal direction and the elasticity matrices for the web $[E]_w$ and flange $[E]_f$ layers become:

$$[E]_w = \frac{t_w}{S}\begin{bmatrix} E & 0 & 0 \\ 0 & 0 & 0 \\ 0 & 0 & 0 \end{bmatrix}, \quad (7)$$

$$[E]_\mathrm{f} = \frac{b_f}{S}\begin{bmatrix} E & 0 & 0 \\ 0 & 0 & 0 \\ 0 & 0 & 0 \end{bmatrix}. \quad (8)$$

The stresses for the layer *i*, i.e. $\{\sigma\}_i = \left\{\sigma_x^i; \sigma_y^i; \tau_{xy}^i\right\}^T$, are obtained from the strains $\{\varepsilon\}$ by multiplying by the layer's elasticity matrix $[E]$:

$$\{\sigma\}_i = [E]_i\{\varepsilon\}_i, i = p, w, f. \quad (9)$$

However, it is important to notice that Eq. 9 represents the average layer cross-section, also including the air. To find the stresses in the stiffener web or flange only, the stresses obtained with the ESL model need to be rescaled accordingly:

$$\sigma_{w,actual} = \frac{S}{t_w}\sigma_w, \quad (10)$$

$$\sigma_{f,actual} = \frac{S}{b_f}\sigma_f. \quad (11)$$

A similar relationship can be applied to obtain the out-of-plane shear stiffness and stresses:

$$\begin{Bmatrix} \tau_{XZ} \\ \tau_{YZ} \end{Bmatrix}_i = \begin{bmatrix} G_{XZ} & 0 \\ 0 & G_{YZ} \end{bmatrix}_i \begin{Bmatrix} \gamma_{XZ} \\ \gamma_{YZ} \end{Bmatrix}_i, i = p, w, f. \quad (12)$$

2.1.3 Relationship between the internal forces and strains

According to ESL-FSDT [62], the element's relationship between homogenised internal forces, strain, and curvatures can be presented as:

$$\begin{Bmatrix} \{\mathrm{N}\} \\ \{\mathrm{M}\} \\ \{\mathrm{Q}\} \end{Bmatrix} = \begin{bmatrix} [\mathrm{A}] & [\mathrm{B}] & [0] \\ [\mathrm{B}] & [\mathrm{D}] & [0] \\ [0] & [0] & [\mathrm{D_Q}] \end{bmatrix} \begin{Bmatrix} \{\varepsilon\} \\ \{\kappa\} \\ \{\gamma\} \end{Bmatrix}, \quad (13)$$

where {N} is the normal force, {M} the moment and {Q} the shear force vectors, which are related to the strain $\{\varepsilon\}$, curvature $\{\kappa\}$, and out-of-plane shear strain $\{\gamma\}$ vectors by multiplying with stiffness matrices. It should be noted here that

because of the selection of the reference plane, the in-plane and bending deformations are coupled. This means that if the B- and D-matrices are neglected, the response is overly simplified. Considering that the reference plane is located on top of the deck plate - see Figure 8 - membrane [A], membrane-bending [B], and bending [D] stiffness matrices are obtained from homogenised constitutive equations by integrating Eq. 9 over the thickness of each layer:

$$[\mathrm{A}] = \int_{-tp}^{0} [E]_{\mathrm{p}}\, dz + \int_{0}^{hw} [E]_{\mathrm{w}}\, dz + \int_{hw}^{hw+hf} [E]_{\mathrm{f}}\, dz, \tag{14}$$

$$[\mathrm{B}] = \int_{-tp}^{0} [E]_{\mathrm{p}}\, z dz + \int_{0}^{hw} [E]_{\mathrm{w}}\, z dz + \int_{hw}^{hw+hf} [E]_{\mathrm{f}}\, z dz, \tag{15}$$

$$[\mathrm{D}] = \int_{-tp}^{0} [E]_{\mathrm{p}}\, z^2 dz + \int_{0}^{hw} [E]_{\mathrm{w}}\, z^2 dz + \int_{hw}^{hw+hf} [E]_{\mathrm{f}}\, z^2 dz, \tag{16}$$

where the integration limits account for the selected reference plane.

In Eq. 13, $[\mathrm{D_Q}]$ represents the out-of-plane shear stiffness, which includes the shear stiffness in the stiffener $\mathrm{D_{Qx}}$ and transverse to the stiffener direction $\mathrm{D_{Qy}}$:

$$\left[\mathrm{D_Q}\right] = \begin{bmatrix} \mathrm{D_{Q}}x & 0 \\ 0 & \mathrm{D_{Q}}y \end{bmatrix}, \tag{17}$$

$$\mathrm{D_{Q}}x = k_{xz}\left(G_p t_p + G_w h_w + G_f h_f\right), \tag{18}$$

$$\mathrm{D_{Q}}y = k_{yz}\left(G_p t_p\right), \tag{19}$$

where G_p is the shear modulus for the plate layer. G_w and G_f are the shear moduli for the web and flange layers, respectively, and are obtained by using the Rule of Mixtures from the Voigt strain approximation, similarly as in Eq. 7 and 8. k_{xz} is the shear correction factor in the *xz*-plane, which relates the average shear stress of the stiffener to the maximum shear stress, i.e. $k_{xz}=(\tau_{xz})_{\mathrm{avg}}/(\tau_{xz})_{\mathrm{max}}$. The shear correction factor k_{yz} follows Reissner-Mindlin plate theory and is taken as 5/6. As a result, an 8x8 stiffness matrix is generated, the components of which are shown in Figure 9.

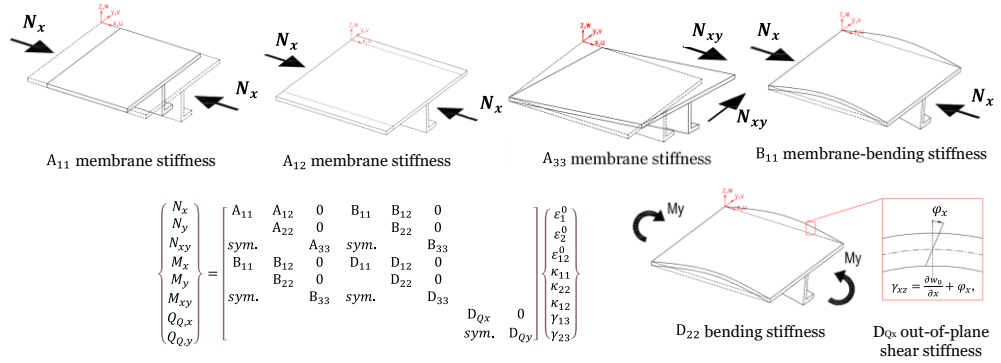

Figure 9. Stiffened panel [A], [B], [D] and [D_Q] stiffness matrix components.

2.1.4 Differential equations

The differential equations are obtained by substituting the constitutive equations into the strain definitions and, further, the result into the equilibrium equations:

$$A_{11}\frac{\partial^2 u_0}{\partial x^2} + A_{12}\frac{\partial^2 v_0}{\partial x \partial y} + B_{11}\frac{\partial^2 \phi_x}{\partial x^2} + B_{12}\frac{\partial^2 \phi_y}{\partial x \partial y} + B_{66}\left(\frac{\partial^2 \phi_y}{\partial y^2} + \frac{\partial^2 \phi_y}{\partial x \partial y}\right) +$$

$$+A_{66}\left(\frac{\partial^2 u_0}{\partial y^2} + \frac{\partial^2 v_0}{\partial x \partial y}\right) = I_0\frac{\partial^2 u_0}{\partial t^2} + I_1\frac{\partial^2 \phi_x}{\partial t^2} + \underline{I_{1,l}\frac{\partial^2 \theta_x}{\partial t^2}}, \tag{20}$$

$$A_{22}\frac{\partial^2 v_0}{\partial y^2} + A_{12}\frac{\partial^2 u_0}{\partial x \partial y} + B_{22}\frac{\partial^2 \phi_y}{\partial y^2} + B_{12}\frac{\partial^2 \phi_x}{\partial x \partial y} + B_{66}\left(\frac{\partial^2 \phi_y}{\partial x^2} + \frac{\partial^2 \phi_x}{\partial x \partial y}\right) +$$

$$+A_{66}\left(\frac{\partial^2 v_0}{\partial x^2} + \frac{\partial^2 u_0}{\partial x \partial y}\right) = I_0\frac{\partial^2 v_0}{\partial t^2} + I_1\frac{\partial^2 \phi_y}{\partial t^2} + \underline{I_{1,l}\frac{\partial^2 \theta_y}{\partial t^2}}, \tag{21}$$

$$D_{Qx}\left(\frac{\partial^2 w_0}{\partial x^2} + \frac{\partial \phi_x}{\partial x}\right) + D_{Qy}\left(\frac{\partial^2 w_0}{\partial y^2} + \frac{\partial \phi_y}{\partial y}\right) + q = I_0\frac{\partial^2 w_0}{\partial t^2} + \underline{I_{0,l}\frac{\partial^2 w_{0,l}}{\partial t^2}}, \tag{22}$$

$$B_{11}\frac{\partial^2 u_0}{\partial x^2} + B_{12}\frac{\partial^2 v_0}{\partial x \partial y} + D_{11}\frac{\partial^2 \phi_x}{\partial x^2} + D_{12}\frac{\partial^2 \phi_y}{\partial x \partial y} + D_{66}\left(\frac{\partial^2 \phi_x}{\partial y^2} + \frac{\partial^2 \phi_y}{\partial x \partial y}\right) +$$

$$+B_{66}\left(\frac{\partial^2 u_0}{\partial y^2} + \frac{\partial^2 v_0}{\partial x \partial y}\right) - D_{Qx}\left(\frac{\partial w_0}{\partial x} + \phi_x\right) - \underline{\frac{\partial M_{xx,l}}{\partial x} + \frac{\partial M_{xy,l}}{\partial y}} =$$

$$= I_2\frac{\partial^2 \phi_x}{\partial t^2} + I_1\frac{\partial^2 u_0}{\partial t^2} + \underline{I_{2,l}\frac{d^2 \theta_x}{dt^2}}, \tag{23}$$

$$B_{22}\frac{\partial^2 v_0}{\partial x^2} + B_{12}\frac{\partial^2 u_0}{\partial x \partial y} + D_{22}\frac{\partial^2 \phi_y}{\partial y^2} + D_{12}\frac{\partial^2 \phi_x}{\partial x \partial y} + D_{66}\left(\frac{\partial^2 \phi_y}{\partial x^2} + \frac{\partial^2 \phi_x}{\partial x \partial y}\right) +$$

$$+B_{66}\left(\frac{\partial^2 v_0}{\partial x^2}+\frac{\partial^2 u_0}{\partial x \partial y}\right)-D_{Qy}\left(\frac{\partial w_0}{\partial y}+\phi_y\right)-\underline{\frac{\partial M_{yy,l}}{\partial y}+\frac{\partial M_{xy,l}}{\partial x}}=$$

$$=I_2\frac{\partial^2 \phi_y}{\partial t^2}+I_1\frac{\partial^2 v_0}{\partial t^2}+\underline{I_{2,l}\frac{d^2\theta_y}{dt^2}}, \quad (24)$$

where the underlined moment and inertia terms are associated with the local bending of the plate between the stiffeners. The inertia terms are found from the following:

$$I_i,=\int_{-tp}^{h}\rho_i\, z^i dz, i=0,1,2, \quad (25)$$

$$I_{i,l},=\int_{-t/2}^{t/2}\rho_i\, z^i dz, i=0. \quad (26)$$

The differential equations that are presented follow the ESL-FSDT theory, but local underlined terms are not supported by commercial FE solvers; see e.g. [85]. Therefore, in practical design these differential equations are difficult to apply for a large-scale design problem and simplifications need to be made. First, the local terms in equilibrium and differential equations are omitted, i.e. the underlined terms are set to zero. As previously explained, this can be achieved by applying the Rule of Mixture and smearing the stiffeners to equivalent plate properties; see Eq. 7 and 8. Another simplification can be made with the first- and second-order rotary inertia terms I_1 and I_2, which consider the z-coordinate mass distribution of the element. Since the mass of the deck plating and outfitting is significantly higher than the mass of the secondary stiffeners, the layer-wise mass distribution of the stiffened panel is negligible, and the mass can be concentrated into the reference plane nodes. These simplifications will bring significant computational savings and commercial laminate shell elements can be used. In most of the ship design analysis, these simplifications are justified. However, in some local design problems the plate bending response between the stiffeners needs to be recoupled with the ESL-solution. For response analysis under lateral loads, [P1] showed that a super-positioning solution can be applied. For vibration analysis, the interaction between local and global effects can be considered using the correction methods presented in [P2] or [P3]. The methods are discussed in more detail in Chapter 3 and Chapter 4.

2.2 Modelling primary beams in the equivalent element model

In thesis-related case studies, the primary beams such as girders and web frames are usually modelled using a CBEAM element, which includes extension,

torsion, bending in two perpendicular planes, and the out-of-plane shear response. By default, the beam element's reference axis is at its neutral axis, which is incorrect when it is part of a ship structure. Therefore, the beam elements need to be offset as shown in Figure 8. The element's membrane [A], membrane-bending [B], and bending [D] stiffness matrices, together with offset, can be described with the following matrix forms:

$$[ABD'] = \begin{bmatrix} 1 & 0 \\ d_{offs} & 1 \end{bmatrix} \begin{bmatrix} A & 0 \\ 0 & D \end{bmatrix} \begin{bmatrix} 1 & d_{offs} \\ 0 & 1 \end{bmatrix} = \begin{bmatrix} A & Ad_{offs} \\ Ad_{offs} & D + Ad_{offs}^2 \end{bmatrix} \quad (27)$$

In most cases this T-girder discretisation gives very good correspondence with the fine mesh results, where the web is modelled using a shell and flange with beam elements. However, at higher deck structure vibration modes the accuracy starts to decrease [P5]. This is due to the fact that in a beam element there is no coupling between the web and flange and the angle of torsional rotation at the interface node corresponds to the angle of the shear centre of the beam's cross-section. In such cases, primary beams should be represented using fine mesh modelling principles [11].

3 Quasi-static analysis

3.1 Primary response level [P1]

The equivalent element that was developed is validated for primary hull girder response analysis with a commonly used box-beam ship under four-point bending in [P1]. Excellent agreement with 3D fine mesh results is observed. However, as several research studies have shown, significant interaction between the hull and superstructure decks occurs in passenger ships; see e.g. [24], [25], [30], [31]. Therefore, in this thesis, as well as in [P4] and [P5], a more advanced model of a prismatic cruise ship is used; see Figure 12. Despite the fact that the ship hull shape is not represented, this generic FE model provides sufficient accuracy and acceptable difference compared to a full FE model; see [45]. The length of the vessel is L=286.944 m, the breadth B=35.8 m, and the draught T=8.05 m. The ship is made of steel, with a Young's modulus of 206 GPa, Poisson ratio of 0.3, and density of 7850 kg/m^3. She has 13 decks with a total height of 43.7 m. The deck plating stiffener spacing is 640 mm. The frame and web frame spacings are 854 mm and 2562 mm, respectively. Depending on location, the thickness of the plating varies from 5 to 16 mm, and it is reinforced with HP profiles from 100x6 to 180x8. A typical girder size in the superstructure part is T-440x7+FB150x10 and in the hull section T-530x7+FB150x10. Fire bulkheads are located at every 40.992 m and they are made of 6-mm steel plate, stiffened HP-120x6 profiles and girders T-250x8+150x10. The main frame of the ship is shown in Figure 10.

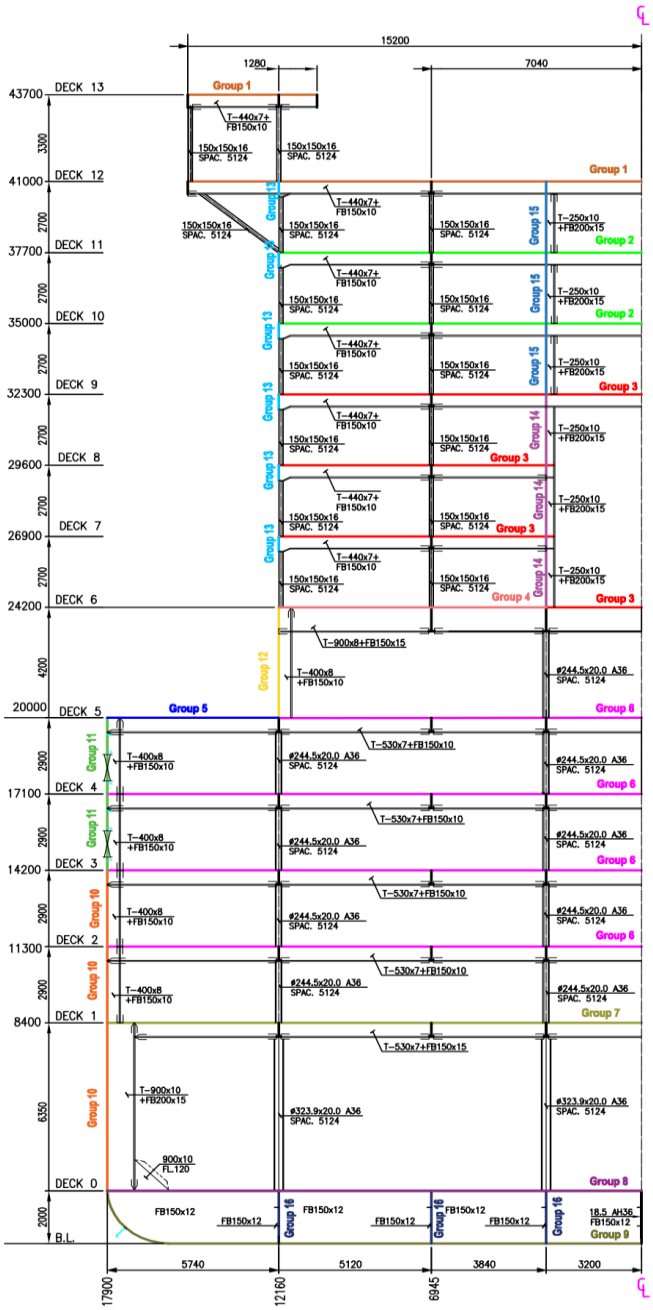

	Used scantlings for static and vibration analysis
Group 1:	t=12.0/HP120x6/S=640
Group 2:	t=6.0/HP120x6/S=640
Group 3:	t=5.0/HP100x6/S=640
Group 4:	t=8.0/HP100x6/S=640
Group 5:	t=10.0/HP120x6/S=640
Group 6:	t=5.5/HP100x6/S=640
Group 7:	t=6.0/HP100x6/S=640
Group 8:	t=13.0/HP180x8/S=640
Group 9:	t=16.0/HP180x8/S=640
Group 10:	t=16.0/HP160x7/S=725
Group 11:	t=16.0/HP160x7/S=650
Group 12:	t=10.0/HP120x6/S=675
Group 13:	t=15.0
Group 14:	t=7.0/HP120x6/S=675
Group 15:	t=7.0/HP120x6/S=675
Group 16:	t=9.5/FB150x12/S=666

Figure 10: Prismatic ship main frame drawing with optimisation groups [P4].

The hull is loaded with vertical bending moment in sagging and hogging loading condition. It is a sum of still water- and wave-induced bending moments, which are calculated using the classification society rules [86]. In still water, a typical cruise ship is in hogging condition, i.e. the weight loads in the aft and fore parts are higher than the buoyancy forces. Therefore, the sagging still water bending moment is taken as zero. The maximum design moment occurs amidships and the total bending moments resulting from hogging and sagging loading conditions are $7.343 \cdot 10^6$ kNm and $-4.616 \cdot 10^6$ kNm, respectively. The moments are generated in the FE model by applying cosine shape pressure to the ship bottom elements; see Figure 11:

$$P = P_{max} \cos\left(\frac{x\pi}{0.5L}\right), \tag{28}$$

where the maximum pressure P_{max} for hogging and sagging condition is 49.2 kPa and -30.94 kPa, respectively. This type of loading will create the highest moment amidships and the highest shear force at the positions $L/4$ and $3L/4$.

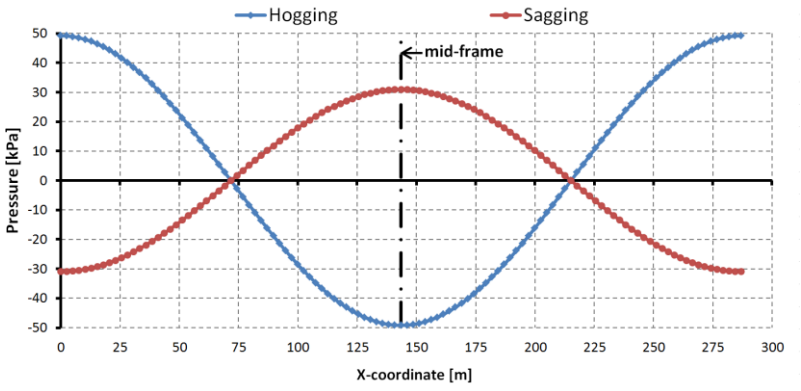

Figure 11: Loading for the prismatic ship bottom structure.

Two types of equivalent element models were created and because of the hull symmetry, only a quarter of the prismatic ship was modelled. The structural continuity of the ship was established by applying symmetric boundary conditions; see Figure 12. In the first type, named the ESL model, stiffened panels are modelled using ESL-FSDT that has been presented. In the second, named the A-matrix model, only the membrane stiffness of the stiffened panels is considered. This is a common simplification for creating a coarse mesh global FE model; see e.g. [13], [23]. Typically, a lumped approach is used [13]. However, in practice it has several disadvantages since a significant number of extra properties need to be created, which will increase the modelling and postprocessing time. As [P5] showed, using a two-layer laminate element instead is a more convenient technique. The first, isotropic, material layer represents the deck plating and the second, orthotropic, material layer the stiffeners, which are smeared evenly along the plating and have stiffness properties in one direction. The layer thickness, t_s, is found by dividing the cross-section area of the stiffener, A_s, by the stiffener spacing, S:

$$t_s = \frac{A_s}{S}, \tag{29}$$

The FE analysis was carried out using the Nastran 2020.1 software and the pre- and post-processing was performed with FEMAP 2020.2. Three different mesh densities are used for the A-matrix and ESL theory-based models: one, two and four elements per web frame spacing; see Figure 13. Laminate elements are created using NX Nastran PCOMP (Layered Composite Element Property),

where the plate layer is described using MAT1 (isotropic) and the stiffener layer(s) with a MAT8 (planar orthotropic) material model. On the basis of the defined PCOMP entity, A, B, D, and D_Q stiffness components according to Eq. 4,7, and 8 and Eq. 18-19 are defined and, according to Eq. 13, represented using one equivalent PSHELL property, which is applied for the four-node CQUAD4 shell element. The results obtained are validated with a 3D fine mesh model, which is created according to the recommendations given in [36]. Plating, stiffener, and girder webs are modelled using QUAD4 shell elements. Offset beam elements (CBEAM) are used to represent the flanges of the stiffeners and girders. The general mesh size is 300 mm, which means two elements between stiffeners, two elements per girder web, and one element per stiffener web height. Around the window openings the mesh size is 50 mm, which corresponds to the classification rule requirements [13].

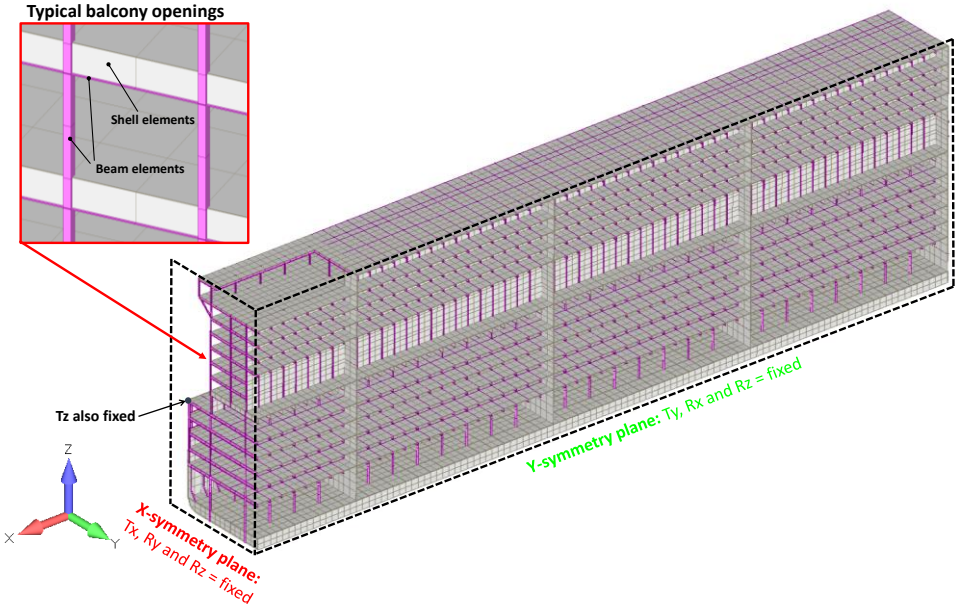

Figure 12: Prismatic FE model of a modern cruise ship with applied boundary conditions.

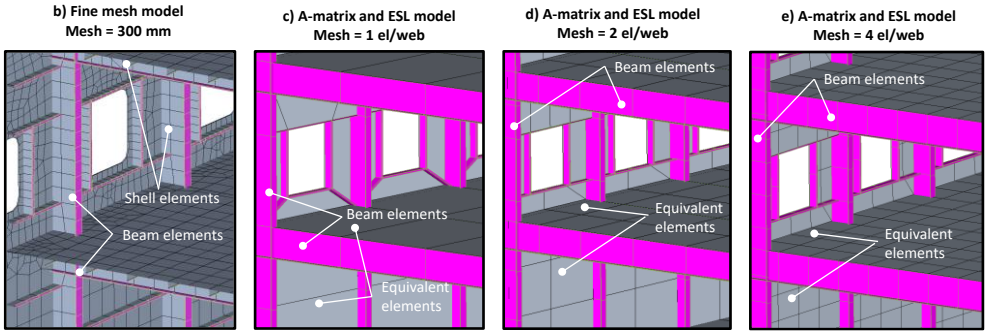

Figure 13. Mesh size of (a) fine mesh model, (b) one element, (c) two elements, and (d) four elements per web frame spacing.

The results obtained from the A-matrix and ABD-matrix ESL models are very similar; see Figure 14, Figure 15, and Figure 16 and both models are suitable for describing the passenger ship hull-superstructure interaction. This indicates that in hull girder bending, the stiffened panels are mostly under membrane forces and membrane bending effects are negligible. This corresponds to the findings for a flat stiffened panel in [4], [50]. The results obtained also show that one element per web frame is already a sufficient mesh size to capture the global behaviour with reasonable accuracy; see Figure 15 and Figure 16. However, to investigate the stress distribution between the web frames or decks with higher accuracy, as well as stress concentrations resulting from openings or structural discontinuities, a finer mesh needs to be used.

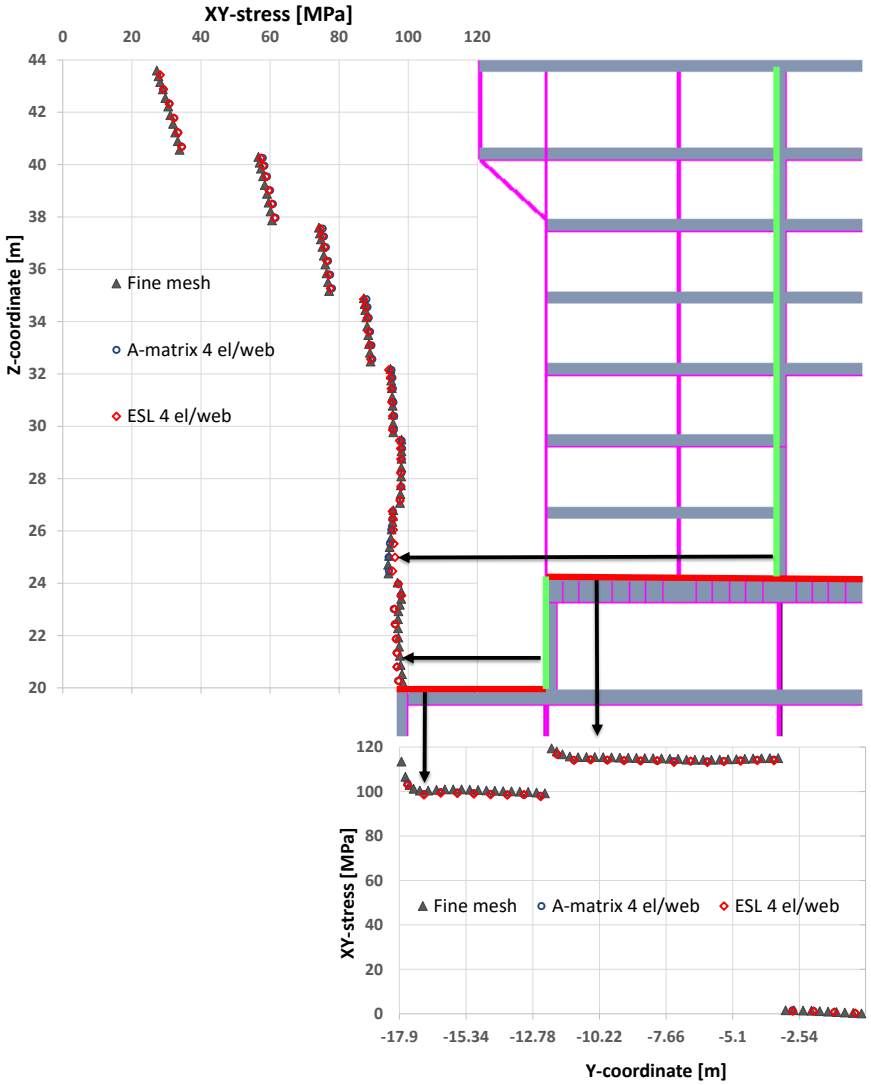

Figure 14: Prismatic ship XY-shear stresses in the recess area, x=*L*/4.

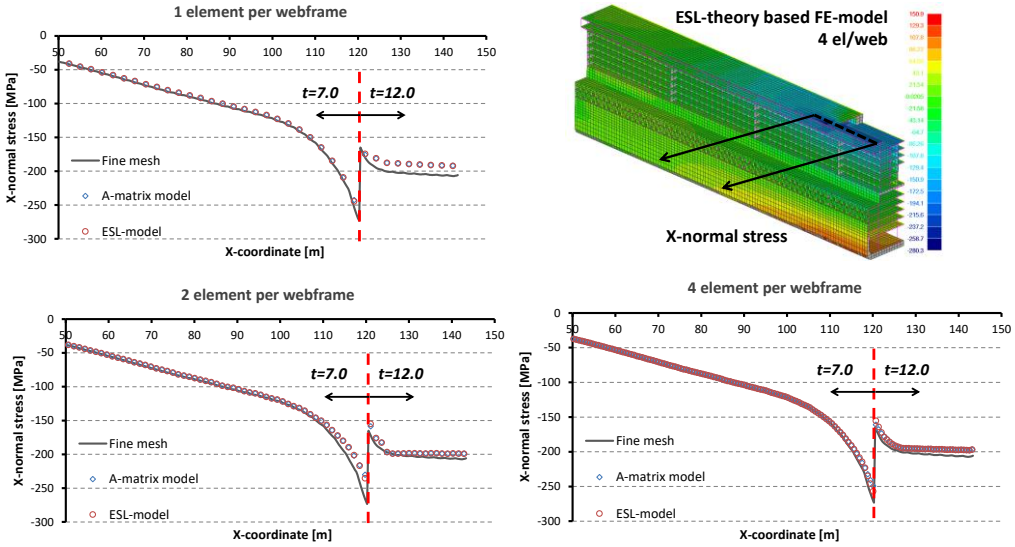

Figure 15: X-normal stresses for ESL and A-matrix models.

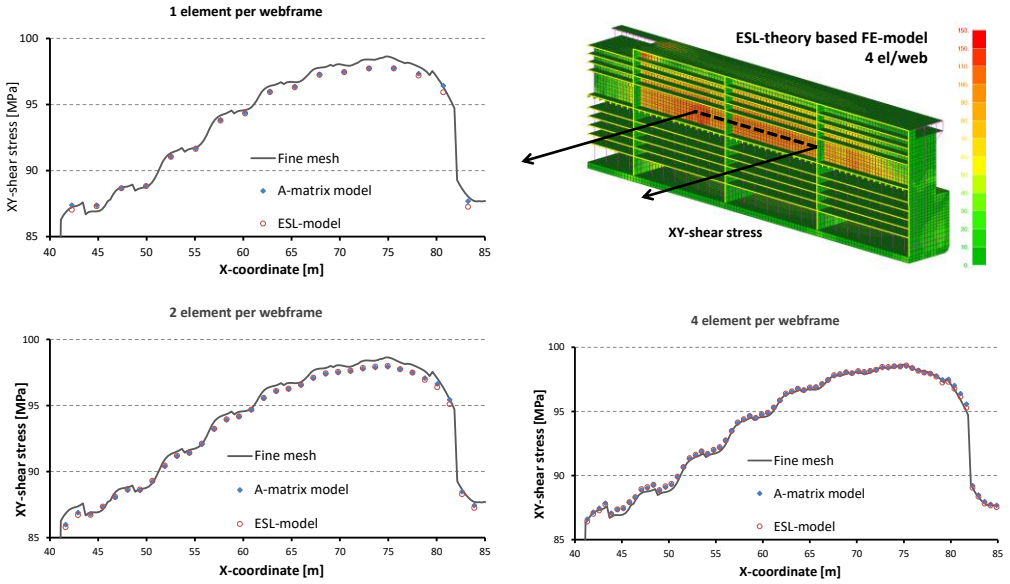

Figure 16: XY-shear stresses for ESL and A-matrix models.

3.2 Secondary and tertiary response level [P1]

To demonstrate the feasibility of the ESL-theory-based equivalent element for secondary- and tertiary-level response analysis, part of the prismatic ship superstructure deck structure, shown in Figure 17, was analysed separately under a lateral pressure of 2.0 kPa. The size of the model in the length direction is four web frame spacings and structural continuity is established using symmetric boundary conditions (BC). Fixed BC were applied to nodes where structural members are connected to the upper and lower deck structure. The thickness of the deck plating is 6.0 mm, and it is stiffened using HP 120x6 profiles with a spacing of 640 mm. The deck T-girder size is T-440x7+150x10 and the web frame spacing 2562 mm. Pillars (RHS-150x150x12.5) are located at

every second frame. All structural parts are made of steel with a Young's modulus of 206 GPa, Poisson ratio of 0.3, and mass density of 7850 kg/m^3. ESL models were created using three different mesh densities: two, four, and 16 elements per web frame spacing; see Figure 18. Validation was performed using a 3D fine mesh model, created according to recommendations given in [36]. A general mesh size of 150 mm is used, which gives four elements between stiffeners and 16 elements per web frame spacing.

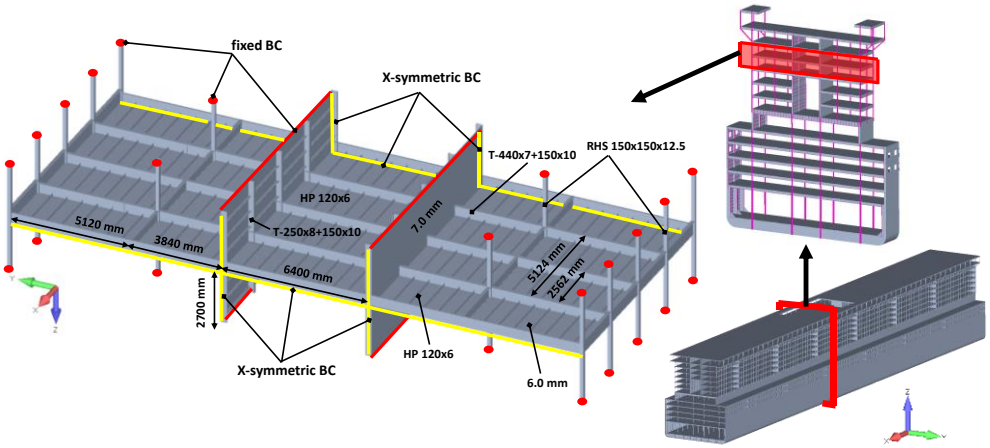

Figure 17 Local cabin area model with scantlings and applied boundary conditions (BC).

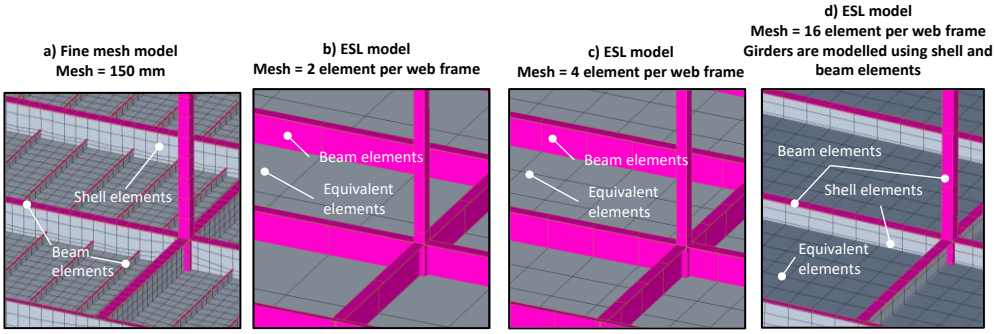

Figure 18. Mesh size of (a) fine mesh model, and (b) two elements, (c) four elements, and (d) 16 elements per web frame spacing in the ESL theory-based equivalent element model.

The deflection of the deck structure along the stiffener is shown in Figure 19. As can be seen, the deflection can be captured with excellent accuracy if the mesh density is at least four elements per web frame spacing. Figure 20 and Figure 21 present the x-directional normal stresses in the mid-surface of the deck plate. This stress component is caused by the stiffener bending together with the deck plating. Both the shape and stress magnitude are generally predicted with good accuracy. The highest error occurs close to the stiffened panel boundaries, as in the fine mesh model the stiffener and T-girder web connection is locally stiffer than in the homogenised ESL model. Additionally, a second limitation occurs in local stress analysis. The homogenisation applied

assumes that the stiffener spacing is infinitely small and thus the deck plating is fully effective, which means that the effects of shear lag on stress distribution cannot be correctly represented. As can be seen from Figure 21, the fine mesh model stresses are slightly higher close to the stiffeners and lower at the middle of the plate, while in the ESL model this oscillation is missing, and average values are presented. However, this small oscillation does not influence the bending behaviour of the stiffener significantly and the stresses in the stiffener members can still be accurately captured; see [P1]. Furthermore, under later loads the local plate bending stresses between the stiffeners are much higher compared to the stress difference resulting from effective breadth; see Figure 21 vs. Figure 25. In addition, as the previous chapter showed, the homogenisation is justified in hull girder response analysis, where the normal forces in the deck plating are evenly distributed along the stiffener spacings. However, this limitation becomes intolerable in limit state analysis, where noticeable force re-distribution occurs [87], or when welding distortions need to be considered [4].

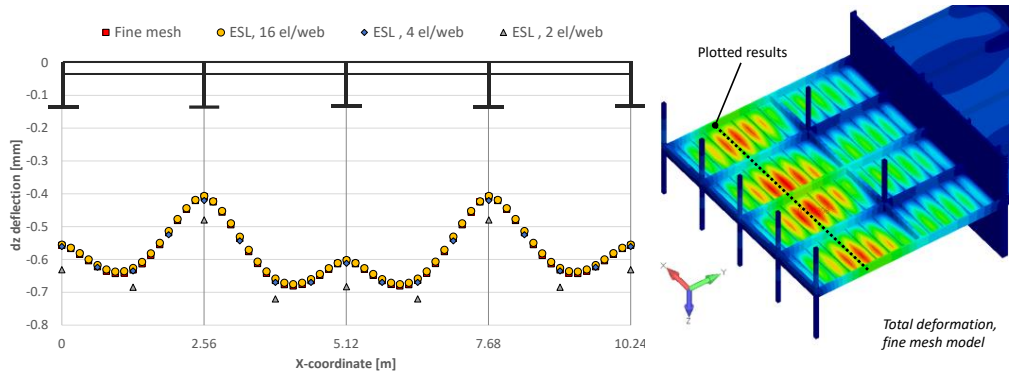

Figure 19. Deflection of the deck structure along the stiffener under uniform pressure of 2 kPa.

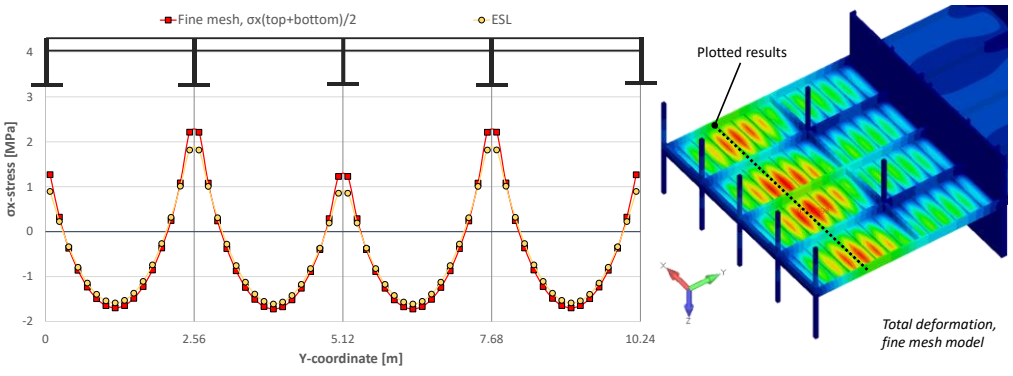

Figure 20. Deck plating σ_X stresses resulting from stiffener column bending, i.e. stiffener bends together with deck plating, at y=-9.6 (along the stiffener)

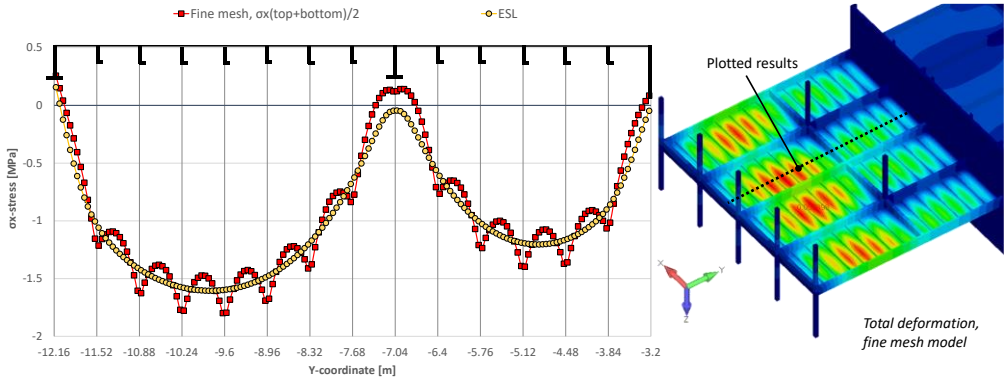

Figure 21. Deck plating σ_x stresses resulting from stiffener column bending, i.e. stiffener bends together with deck plating, at x=3.843 (at the middle of the stiffened panel)

To illustrate the need of having the element offset according to Figure 8, the results are additionally compared with the ESL model, where the element reference plane corresponds to the geometrical mid-plane, as in [23], [52], [53], [56]. Additionally, in these ESL models, T-girders are modelled as in the fine mesh model using shell elements for web and beam elements for flanges [11], to achieve better comparison between the fine mesh results. As can be seen, the offset has a significant effect on the results. A similar shape is obtained, but the values are 10-20% higher; see Figure 22. In Figure 23 the stresses at the transversal girder and on the nearby deck plating resulting from lateral pressure are presented. Between ESL and fine mesh excellent correspondence is obtained, but the stress distribution angle is different when the reference plane is located at the geometrical mid-plane in the web layer. Thus, the interaction between the girder and the stiffened panel is not correctly represented as the laminate element plate layer is wrongly coupled with the bending of the girder and plate.

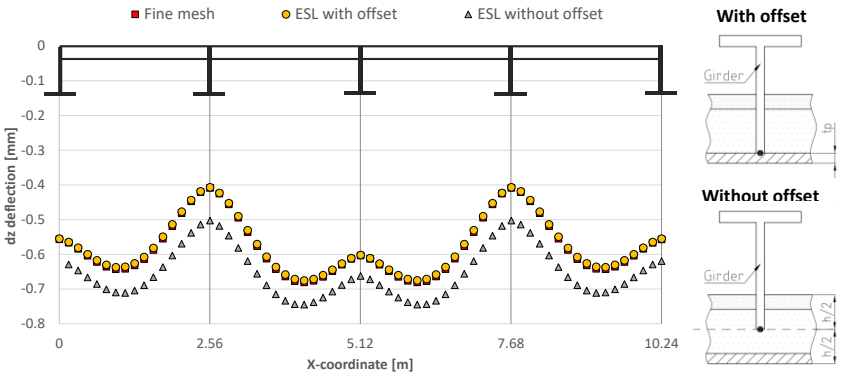

Figure 22. Deflection of the deck structure when the ESL reference plane is offset and when it corresponds to the geometrical mid-plane (without offset).

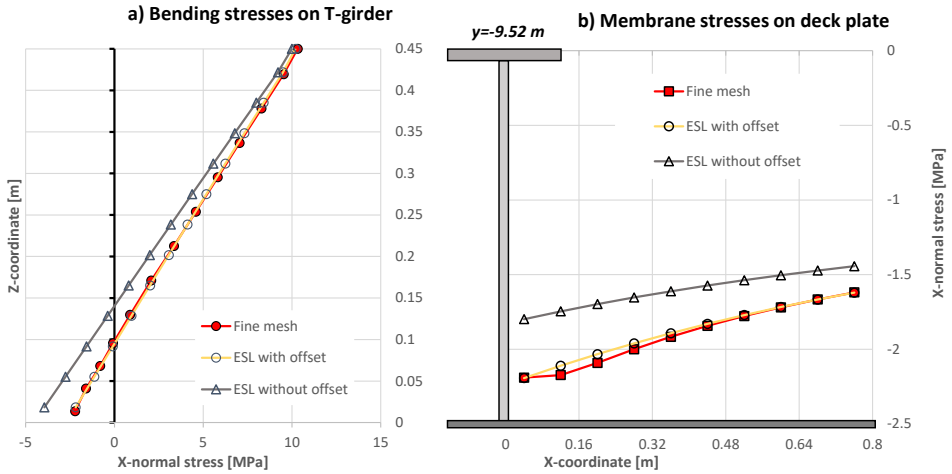

Figure 23. Stresses on (a) the transversal T-girder web and flange and (b) the deck plating when the ESL reference plane is offset and when it corresponds to the geometrical mid-plane.

To investigate the plate bending response between the stiffeners the ESL homogeneous theory becomes limited and local behaviour needs to be added. In quasi-static analysis, the local plate response between the stiffeners can be considered as a clamped-clamped plate under pure bending, where the normal stress vector $\{\sigma\}_l = \{\sigma_x^l, \sigma_y^l, \tau_{xy}^l\}^T$ is obtained by multiplying the strain vector $\{\varepsilon\}_l$ by the deck plate elasticity matrix $[E]_p$:

$$\{\sigma\}_l = [E]_p\{\varepsilon\}_l. \tag{30}$$

Under pure bending behaviour, the strain vector $\{\varepsilon\}$ is defined as:

$$\begin{Bmatrix} \varepsilon_x \\ \varepsilon_y \\ \varepsilon_{xy} \end{Bmatrix}_l = -z \begin{Bmatrix} \kappa_x \\ \kappa_y \\ \kappa_{xy} \end{Bmatrix}, \tag{31}$$

where $\{\kappa\}$ is the curvature. The total $\{\sigma\}_{tot}$ top and bottom deck plate stresses are obtained by simply adding the local plate bending stresses $\{\sigma\}_l$ to the ESL-solution $\{\sigma\}_{ESL}$, i.e:

$$\begin{Bmatrix} \sigma_x^{tot} \\ \sigma_y^{tot} \\ \tau_{xy}^{tot} \end{Bmatrix}_i = \begin{Bmatrix} \sigma_x^{ESL} \\ \sigma_y^{ESL} \\ \tau_{xy}^{ESL} \end{Bmatrix}_i + \begin{Bmatrix} \sigma_x^{l} \\ \sigma_y^{l} \\ \tau_{xy}^{l} \end{Bmatrix}_i, \quad i = \text{t,b}, \tag{32}$$

where t and b represent the top and bottom surfaces of the deck plate, respectively. With a similar approach it is possible to obtain the total deflection and internal force. As Figure 24 shows, after applying the correction, it is possible to extend the validity of the equivalent element and perform the analysis on the tertiary response level as well. In Figure 25, the deck plating stresses in the same location are presented. As can be seen, larger error occurs

in the elements around the stiffened panel boundaries, but in the rest of the cross-section excellent correspondence with the fine mesh results is obtained. This introduces significant time savings, since the global FE model of the ship can also be utilised for strength analysis under various lateral loads, such as wave, tank, or wheel pressure, which otherwise need to be calculated using tedious analytical methods.

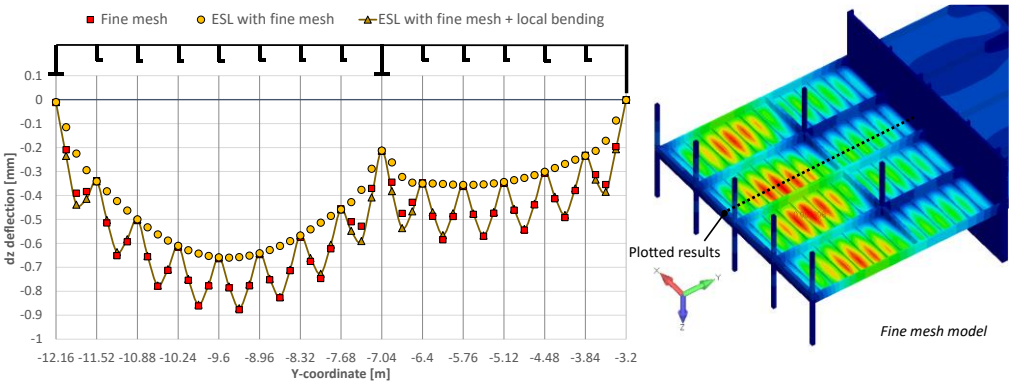

Figure 24. Deflection of the deck structure across the stiffeners under uniform pressure of 2 kPa.

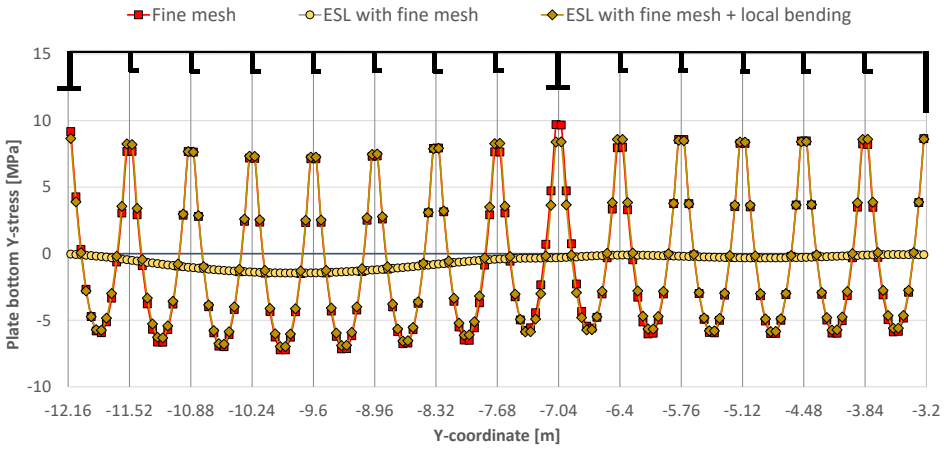

Figure 25. Deck plating bending stresses under uniform pressure of 2 kPa.

4 Vibration analysis

4.1 Ship hull girder free vibration [P1 & P5]

To evaluate a ship's wave-induced vibration performance, precise calculation of the global natural frequencies of hull girder is required [16], [17]. Therefore, the equivalent element that was developed is tested for mode analysis of a simple box-like ship in [P1] and for a more complex cruise ship structure in [P5]. A similar prismatic cruise ship model to that shown in Figure 12 was used, but instead of a quarter of a vessel, a full-size ship was modelled and analysed for various mesh sizes, i.e. one, two and four elements per web frame spacing. Hull girder natural frequencies were calculated up to 7.0 Hz and only the dry modes were considered to avoid any additional disturbance resulting from added water effects. The validation was performed using a 3D fine mesh model. The results were additionally compared with a model where only a stiffened panel membrane property, i.e. the A-matrix, is considered and the mesh size is one element per web frame. This is a common technique for creating a coarse mesh global FE model, which is also recommended by the classification rules [13]. The mode shapes that were obtained are presented in Figure 26 and the values listed in Table 1.

The results indicate that one element per web frame spacing is already a sufficient mesh size to capture the global hull girder vibration modes with less than a 1% difference compared to the fine mesh model. As in the quasi-static analysis, the results obtained from the A-matrix model are also very similar to those from the ABD matrix-based ESL and fine mesh models. Thus, to analyse hull girder modes and perform wave-induced vibration analysis, it is already sufficient to include only the membrane stiffness of the stiffened panel. However, this assumption is valid for relevantly long vessels, in which global modes occur at significantly lower frequencies compared to the local structure modes.

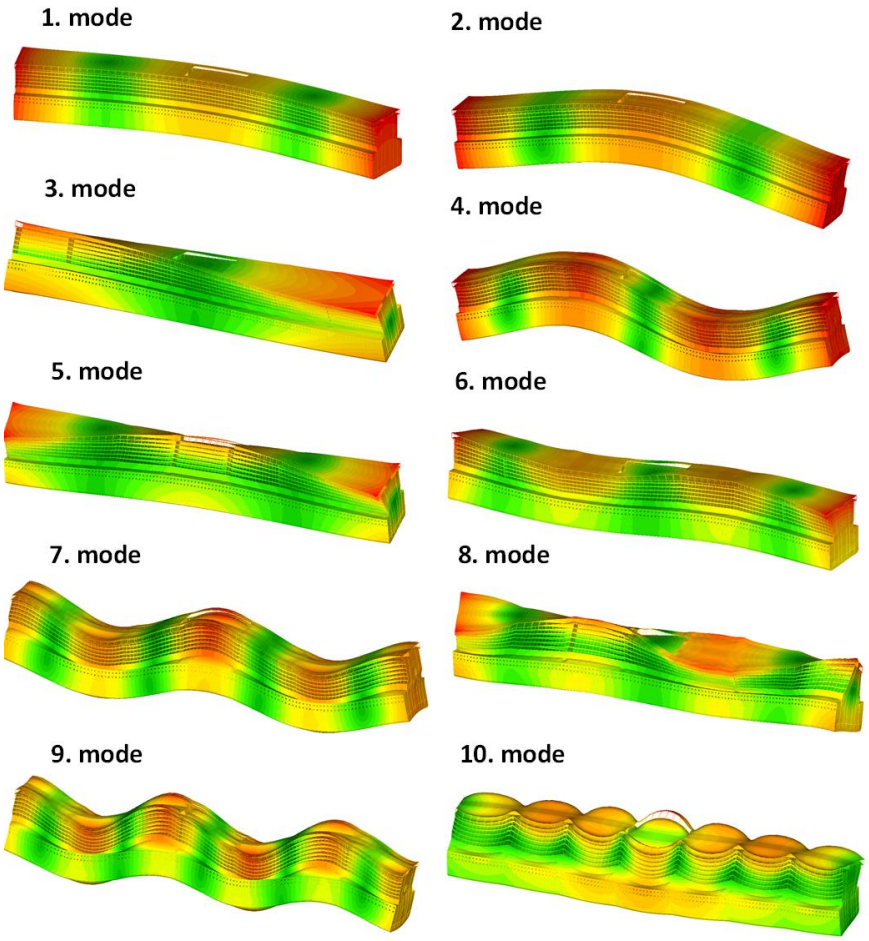

Figure 26. Calculated first ten natural frequency dry modes of prismatic ship (fine mesh model) [P5].

Table 1. Natural frequencies [Hz] of first ten dry modes of the fine mesh, A-matrix and ESL theory-based models [P5].

	Fine mesh	1 el/web A-matrix	diff. [%]	1 el/web ABD-matrix	diff. [%]	2 el/web ABD-matrix	diff. [%]	4 el/web ABD-matrix	diff. [%]
1. mode	1.89	1.89	-0.1	1.89	-0.1	1.89	0.1	1.89	-0.1
2. mode	1.96	1.97	0.0	1.97	0.1	1.96	-0.2	1.95	-1.0
3. mode	2.13	2.12	-0.7	2.12	-0.5	2.10	-1.5	2.07	-2.8
4. mode	3.56	3.54	-0.5	3.55	-0.3	3.53	-0.8	3.49	-1.9
5. mode	4.10	4.08	-0.5	4.09	-0.2	4.05	-1.1	4.01	-2.1
6. mode	4.46	4.46	-0.1	4.46	0.0	4.46	0.0	4.45	-0.2
7. mode	5.15	5.12	-0.5	5.13	-0.4	5.10	-0.8	5.05	-1.8
8. mode	6.05	6.02	-0.5	6.04	-0.3	6.00	-0.8	5.97	-1.4
9. mode	6.41	6.37	-0.7	6.38	-0.5	6.35	-0.9	6.30	-1.7
10. mode	6.78	6.80	0.3	6.83	0.8	6.76	-0.2	6.75	-0.5

4.2 Free vibration of stiffened panels [P2]

In [P2] a simplified method for calculating the half-wave modes of stiffened panels is presented. This allows the equivalent element theory presented here also to be utilised in cases where the global and local vibration modes of the stiffened panel interact. According to [P2], a single-degree-of-freedom spring-mass system can be used to represent each stiffener and the plate between them; see Figure 27a. By using the averaging approach that is presented, this complicated arrangement can be simplified into a system with two masses and three springs as shown in Figure 27b. The mass m_s represents the mass of all the stiffeners and m_d represents the mass of all the plates without the stiffeners. The spring k_s represents the bending of the stiffeners, k_d represents the bending of the plate relative to the stiffeners, and k_w the bending of the plate relative to the boundaries.

While the mass components of this system are known, the stiffness components of the system presented in Figure 27b are unknown. They can be found on the basis of the following assumptions. The angular frequency of the ESL model that is obtained, i.e. ω_{ESL}, represents a situation, in which the spring k_d is infinitely stiff, as the local plate deformation does not exist. For that reason, the system becomes a single-DOF oscillator with a mass m_s+m_d and stiffness k_s+k_w. On the other hand, ω_l represents the situation in which only plate vibration between the stiffeners occurs. Hence, k_s is infinitely stiff and the remaining part is thus a single-DOF oscillator with a mass m_d and stiffness k_d + k_w. One additional equation is needed in order to find these three unknowns. As the deck plate is located between the stiffeners and web frames, the stiffness ratio between the springs k_d and k_w can be approximated using the envelope method. k_w is proportional to the stiffener spacing S and k_d is proportional to the stiffener length L. After these three assumptions are combined, the following relations are obtained [P2]:

$$\begin{cases} k_s + k_w = (m_d + m_s)\omega_{ESL}^2 \\ k_d + k_w = m_d\omega_l^2 \\ k_w = \frac{S}{(2L-S)\left(k_d^{-1}+k_s^{-1}\right)} \end{cases}. \tag{33}$$

While ω_{ESL}^2 can be found from the ESL-theory based model, local terms need to be calculated separately using analytical formulae or the sub-modelling technique. On that basis, an averaged local plate frequency ω_l for a stiffened

panel with a number of stiffeners n_s for the global mode number m can be found. For a pinned panel it is:

$$\omega_l = \sqrt{\frac{2m\omega_{cp}^2+(n_s+1-2m)\omega_{cc}^2}{n_s+1}} \tag{34}$$

and for a clamped panel:

$$\omega_l = \sqrt{\frac{(2m-2)\omega_{cp}^2+(n_s+3-2m)\omega_{cc}^2}{n_s+1}}, \tag{35}$$

where ω_{cc} is the natural frequency of a clamped-clamped plate, which represents the plate vibration between the stiffeners and ω_{cp} for a pinned-clamped plate, a condition where the half-wave of the global mode changes its direction; see Figure 27a.

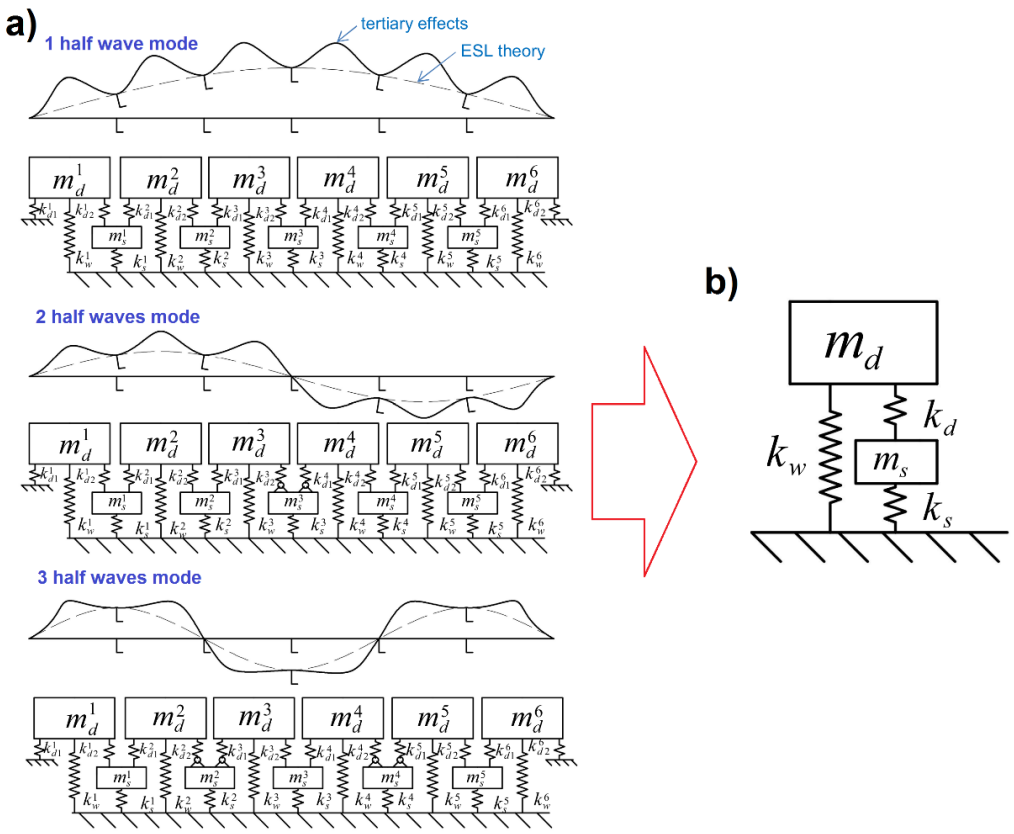

Figure 27. (a) Complete spring-mass and (b) the simplified system for a stiffened panel [P2].

When the stiffness components are known, the corrected squared angular frequency of the stiffened panel ω_{panel}^2 can be found by calculating the lowest eigenvalue of the mass normalised stiffness matrix [88] of the spring-mass system presented in Figure 27b:

$$\left[\tilde{\mathrm{K}}\right] = \left[[\mathrm{M}]^{-1}[\mathrm{K}]\right], \tag{36}$$

where the mass matrix [M] is:

$$[\mathrm{M}] = \begin{bmatrix} m_s & 0 \\ 0 & m_d \end{bmatrix}, \tag{37}$$

and the stiffness matrix is:

$$[K] = \begin{bmatrix} k_s + k_d & -k_d \\ -k_d & k_d + k_w \end{bmatrix}. \tag{38}$$

After Eq. 36 has been solved, the smallest eigenvalue is found from the following relation:

$$\omega^2_{panel} = \frac{b - \sqrt{b^2 - 4ac}}{2a}, \text{ where} \tag{39}$$

$$a = m_d m_s,$$

$$b = k_d m_d + k_s m_d + k_d m_s + k_w m_s,$$

$$c = k_s k_w + k_d k_s + k_d k_w.$$

The method is applied for various pinned and clamped stiffened panels; see Figure 28. The natural frequencies for one half-wave modes as a function of deck plate thickness are presented in Figure 29. In thinner plates, the plate vibration between the stiffeners is more dominant and thus the averaged natural frequency of the sub-models is similar to that of the stiffened panel. When the deck plate thickness increases, the averaged natural frequency of the sub-models gets higher and does not influence the panel solution anymore. At the same time the ESL theory without correction starts to follow the fine mesh results better. Between both extremes the correction method that was developed predicts the natural frequencies of the panel with high accuracy. A similar conclusion can be drawn for a clamped panel with a varying stiffener spacing; see Figure 30.

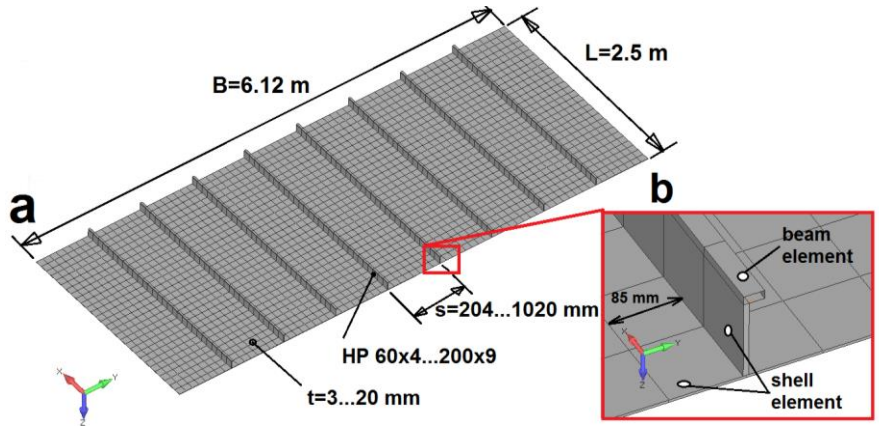

Figure 28. (a) The dimensions of the stiffened panel (mm); (b) mesh density in the fine mesh model [P2].

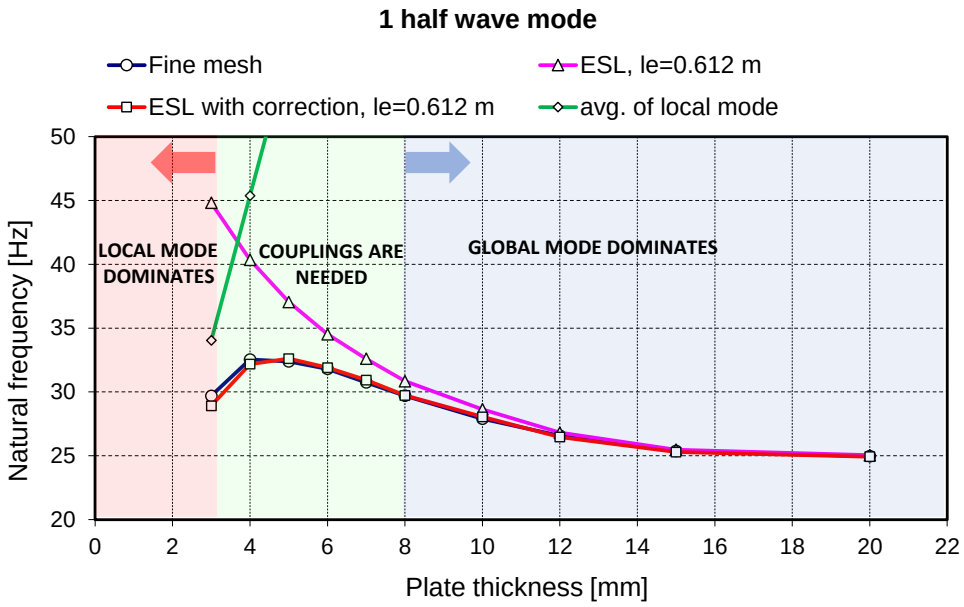

Figure 29. Natural frequencies of one half wave mode of the simply supported panel with varying deck plate thickness [P2].

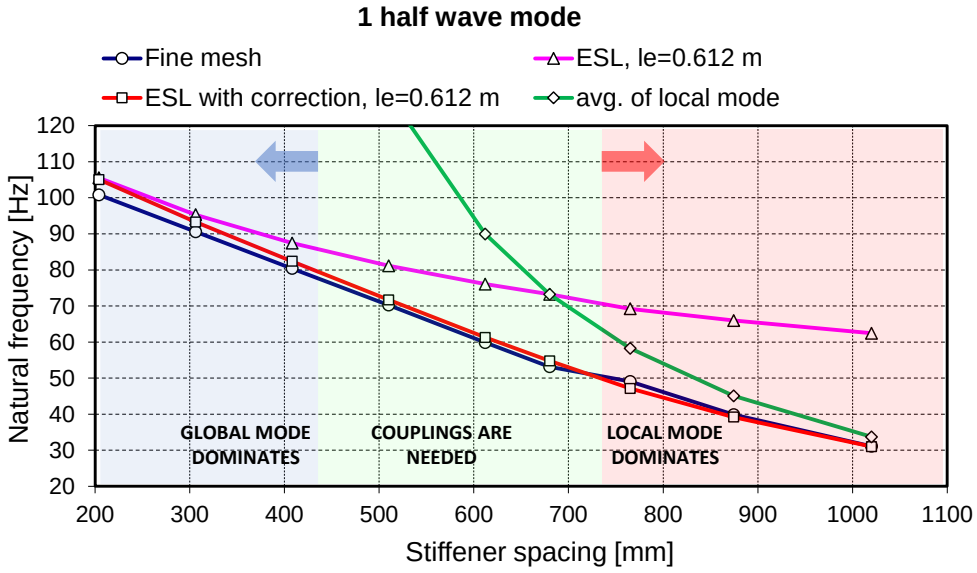

Figure 30. Natural frequencies of one-half wave mode of the clamped panel with varying stiffener spacing [P2].

All the [P2] results are summarised in Figure 31, where the difference between the results of ESL and ESL with correction are presented as a function of the ratio between the natural frequencies of the local plate and ESL theory-based stiffened panel model. During the case studies, ratios from 0.4 to 15 were analysed and, as can be seen, the results follow a similar pattern, which can be expressed by the following power function:

$$ESL_{error,\%} = 31.3\left(\frac{\omega_{local}}{\omega_{ESL}}\right)^{-1.95}, \quad (40)$$

where $ESL_{error,\%}$ is the % difference between the ESL results compared to ESL with correction. ω_{ESL} is the natural frequency of the panel obtained from the ESL model, and ω_{local} is the natural frequency of the plate between the stiffeners.

According to Eq. 35, if the ratio between the natural frequency of the plate between the stiffeners and ESL is less than 2.5, then the error caused by the exclusion of interaction in the natural frequency analysis is within 5%. However, the limit of 2.5 is valid for the calculation of the natural frequency. For forced vibration analysis, where different modes influence each other and the resonance peak also has a certain bandwidth, it is recommended to increase this limit to 3.0, i.e. $\omega<\omega_{local}/3$, to be conservative. Forced vibration is discussed more thoroughly later in Chapter 4.4.

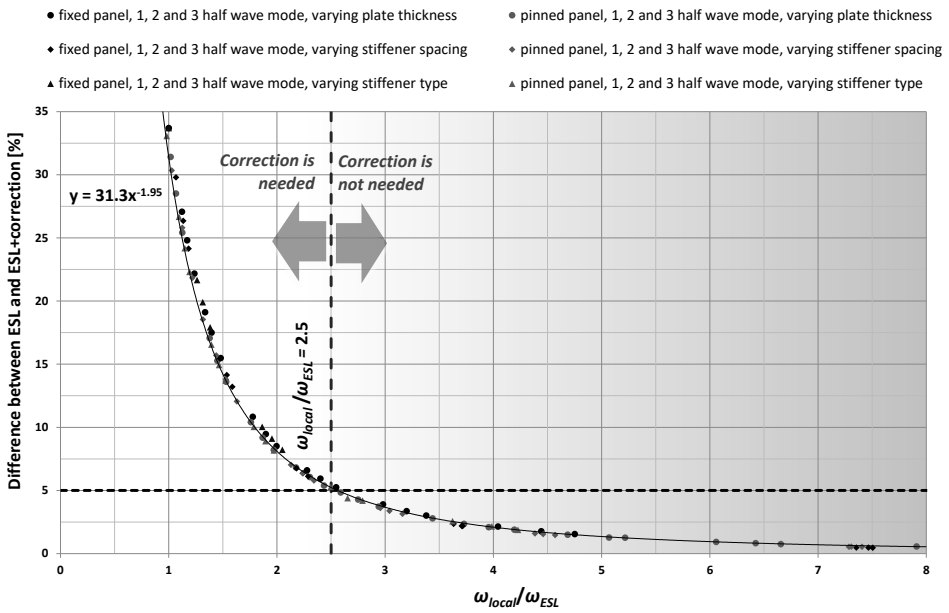

Figure 31. Difference between the results of ESL and ESL with correction as a function of the ratio between the natural frequencies of the local plate and ESL [P5].

4.3 Free vibration of deck structure [P1]&[P3]

The correction method presented in [P2] is limited to a stiffener-plate system only. As ship structures also contain other structural members such as girders, pillars, and bulkheads, a more advanced correction method was developed in [P3], in which the modification of natural frequencies is carried out using the kinetic and strain energies of local deformations. The displacement mode shape

$\Psi_m(x, y, s, \omega_m)$ of the global mode m can be divided into the sum of the global reference plane mode shape $\Psi_{Gm}(x, y)$ and local plate deformation shape $\Psi_{Lm}(x, y, s, \omega_m)$; see Figure 32. The global mode shape is obtained from the ESL model and the local one from an analytical formula or using the sub-modelling technique.

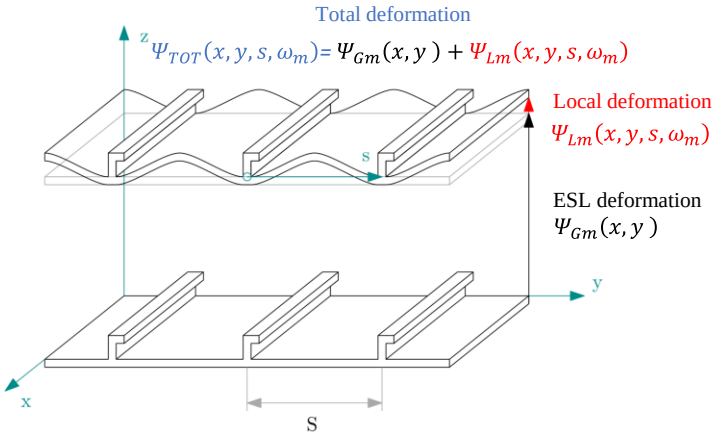

Figure 32. Coordinate system with global and local plate deformation between stiffeners [P3].

A flowchart of the correction method is shown in Figure 33. In each iteration loop, the generalised mass $M_m(\omega_i)$ and generalised stiffness $K_m(\omega_i)$ are calculated, and from these the angular frequency for the next iteration step i+1 is found. Iteration continues until the desired convergence is achieved:

$$\omega_{i+1} = \sqrt{\frac{K_m(\omega_i)}{M_m(\omega_i)}}, if(\omega_i \approx \omega_{i+1}) \rightarrow \omega_m = \sqrt{\frac{K_m(\omega_m)}{M_m(\omega_m)}}. \quad (41)$$

The generalised mass is found from the following equation:

$$M_m(\omega_m) = \frac{2}{\omega_m{}^2 A_m{}^2}\left[T_{Cm}^{peak}(\omega_m) + T_{LR}(\omega_m)\sum_{n=1}^{N}(\alpha_n \Psi_{Gmn}{}^2)\right], \quad (42)$$

where A_m is the generalised amplitude of the mode m and α_n is an effective element area which corresponds to a single node n with the global deformation mode shape Ψ_{Gmn}. $T_{Cm}^{peak}(\omega_m)$ represents the peak value of all the translation kinetic energy of the model, except the z-component of the deck plate; see [P3] for details. $T_{Dzm}(\omega_m, t)$ is the deck plate's z-directional part of the kinetic energy and m_{da} the deck plate mass per area. T_{LR} is a local kinetic energy factor, which represents the kinetic energy of unit deck area under enforced excitation of the unit amplitude of the global reference plane:

$$T_{LR}(\omega_m) = \frac{\omega_m{}^2 m_{da}}{2s}\int_0^s \left(1 + \Psi_{Lm}(s, \omega_m)\right)^2 ds\,, \quad (43)$$

where the coordinate s describes the local distance from the stiffeners; see Figure 32. Considering the assumption that during deck structure vibration,

only the lowest local clamped-clamped mode is active, the mode shape of which, $\Psi_{Lm}(s,\omega_m)$, can be solved by the solution presented in [89], Eq. 43 can be simplified to:

$$T_{LR}(\omega_m) \approx \omega^2 m_{da}\left(\frac{1}{2} + 0.523164\, r_d(\omega) + 0.198239\, {r_d}^2(\omega)\right), \qquad (44)$$

where $r_d(\omega)$ is the dynamic response of the midspan.

The generalised stiffness of the mode m is found from the following equation:

$$K_m(\omega_m) = \frac{2}{{A_m}^2}\left(U_{Cm}^{peak} + U_{LR}(\omega_m)\sum_{n=1}^{N}(\alpha_n {\Psi_{Gm,n}}^2)\right), \qquad (45)$$

where U_{Cm}^{peak} represents the peak value of the strain energy of the uncorrected, i.e. initial ESL model and is found from the following relationship:

$$U_m^{peak} = \frac{1}{2}K_{ESL,m}{A_m}^2 = \frac{{\omega_{ESL,m}}^2}{2}, \qquad (46)$$

$U_{LR}(\omega_m)$ presents the averaged strain energy density of the local deformation of the deck plate induced by unit amplitude enforced excitation of the global reference plane:

$$U_{LR}(\omega_m) = \frac{EI}{2S}\int_0^S \left[\frac{\partial^2[\Psi_{Lm}(s,\omega_m)]}{\partial s^2}\right]^2 ds \approx 99.23127\,\frac{EI{r_d}^2(\omega_m)}{S^4}. \qquad (47)$$

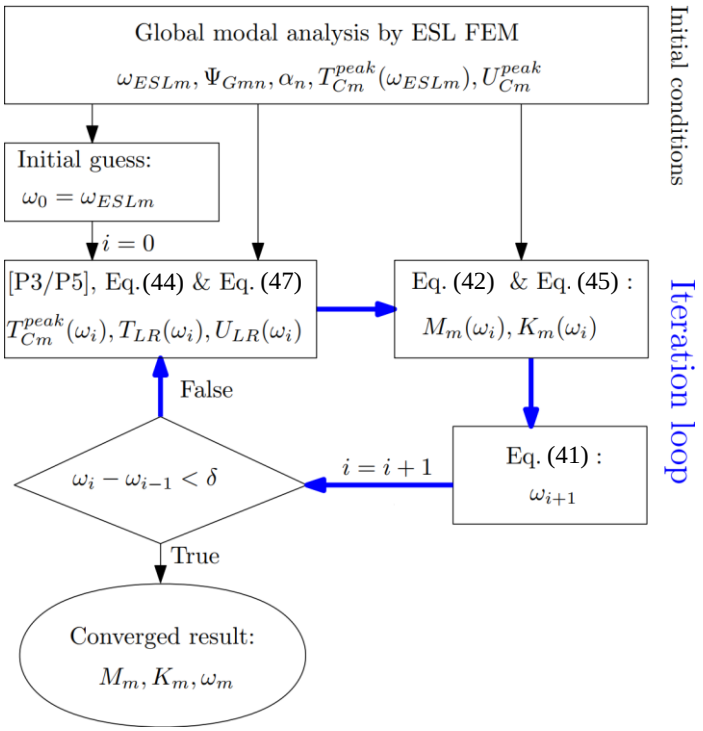

Figure 33. Flow chart of the correction method [P3].

The correction method that was developed is applied for calculating the natural frequencies of a cruise ship deck structure; see Figure 17 and [P5]. The

non-structural mass of 100 kg/m² is used for the deck, with 50% of the mass being carried by the transversal and longitudinal T-girders and the rest by the deck plating. In natural frequency analysis, lumped mass formulation is used, in which the structural and non-structural mass is simply divided between the nodes. According to this schema, a computationally effective diagonal mass matrix is built. The first six modes are analysed using models with various mesh densities. The results are listed in Table 2 and the corresponding mode shapes are shown in Figure 34. As in lateral pressure analysis, one element per web frame spacing is not a sufficient mesh size for representing mode shapes between pillars. When two elements per web frame spacing are used, then good results are also observed without applying correction. This is due to the error cancelling effects of the lumped mass matrix; see [P1] and [P5]. When four or more elements per web frame spacing are used, the error-cancellation effect disappears, and the error of the ESL theory-based model converges between 3 and6%. After the correction is applied, this error is reduced to less than 1%; see Table 2.

Table 2. Natural frequencies of the first six modes in the cruise ship cabin area [P5].

	Fine mesh	ESL, 1 el/web	ESL, 1 el/web with correction	ESL, 2 el/web	ESL, 2 el/web with correction	ESL, 4 el/web	ESL, 4 el/web with correction	ESL, 8 el/web	ESL, 8 el/web with correction
1. mode [Hz]	19.7	17.4	17.1	19.7	19.2	20.3	19.7	20.4	19.8
Error [%]	-	-11.6	-13.4	-0.1	-2.8	3.0	0.0	3.8	0.7
2. mode [Hz]	19.9	17.8	17.5	19.9	19.4	20.6	19.9	20.7	20.1
Error [%]	-	-10.6	-12.4	0.1	-2.7	3.2	0.1	4.0	0.8
3. mode [Hz]	22.8	19.4	18.9	22.3	21.5	23.4	22.5	23.7	22.7
Error [%]	-	-15.0	-17.1	-1.9	-5.5	2.9	-1.4	4.0	-0.4
4. mode [Hz]	22.8	19.4	18.9	22.7	21.9	23.7	22.7	24.0	23.0
Error [%]	-	-14.7	-16.8	-0.2	-3.9	4.2	-0.2	5.3	0.8
5. mode [Hz]	24.6	20.1	19.5	24.5	23.4	25.5	24.2	25.9	24.6
Error [%]	-	-18.5	-20.7	-0.7	-5.1	3.5	-1.7	5.2	-0.2
6. mode [Hz]	24.8	20.0	19.5	24.6	23.5	25.8	24.5	26.1	24.8
Error [%]	-	-19.3	-21.5	-1.0	-5.5	3.8	-1.5	5.1	-0.3

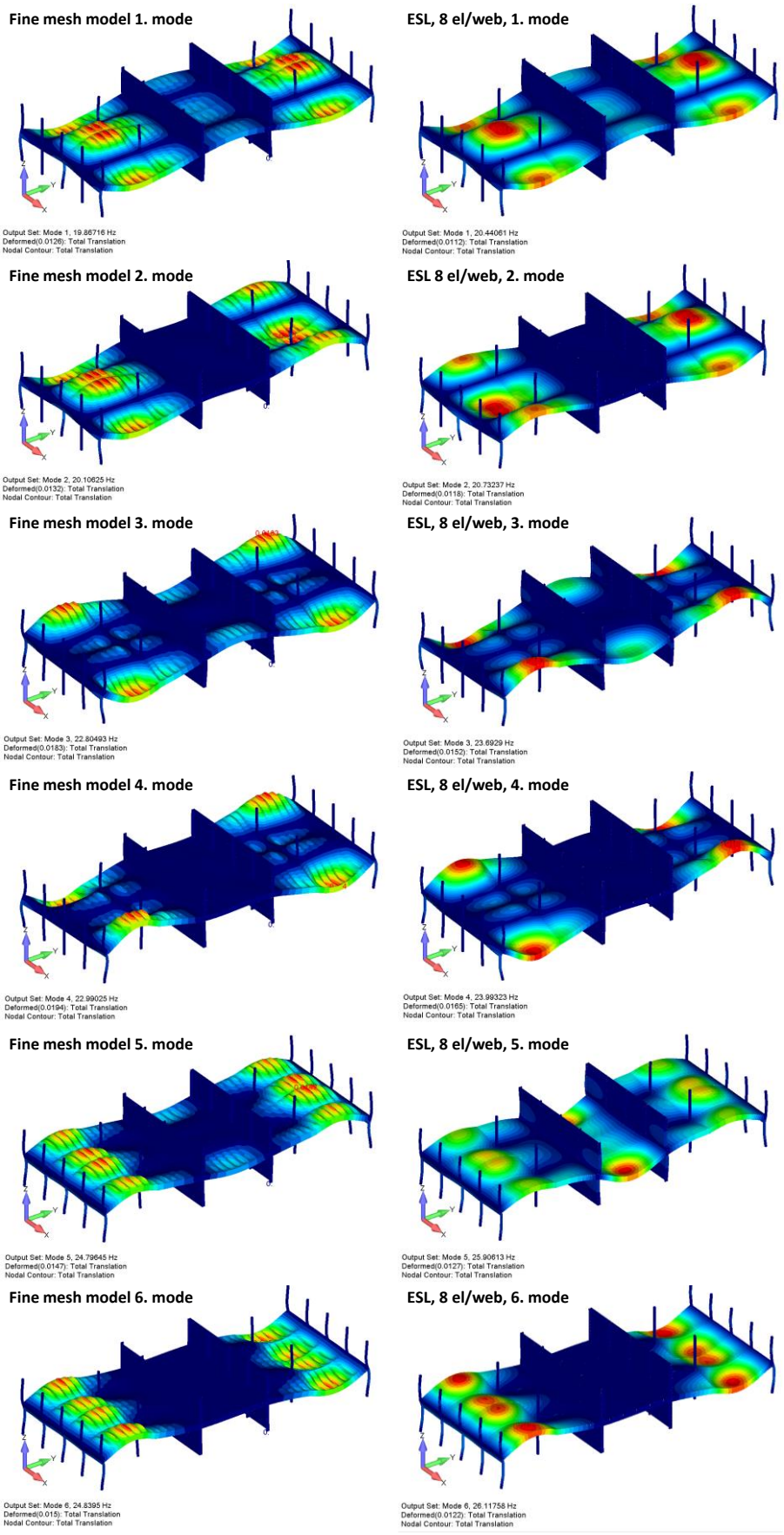

Figure 34. First six vibration modes of 3D fine mesh and ESL model in the cabin area structure [P5].

4.4 Forced vibration response analysis [P5]

The forced response of the complete system can be found by using a modal response calculation method, in which the response of each individual mode is combined. For the mode m, the equation of motion is found from the following relationship:

$$M_m\ddot{U} + C_m\dot{U} + K_mU = F_m \quad (48)$$

where $\ddot{U}$, $\dot{U}$, and U are acceleration, velocity, and displacement vectors, respectively, and M is the structural mass and K the stiffness matrix. F is the generalised force and C is the viscous damping. To calculate the response at the node n, Eq. 48 can be simplified into a single-degree-of-freedom system [90], in which the amplitude for the generalised coordinate $X_{m,n}$ and phase angle ϕ_m for the mode m, at the excitation frequency ω and under a sinusoidal excitation force, $F(t) = F_0 \sin \omega t$, can be found from the following equations:

$$X_{m,n} = \frac{F_n \frac{1}{K_m}}{\sqrt{\left(1-\frac{\omega^2}{\omega_m^2}\right)^2 + \left(2\varsigma\frac{\omega}{\omega_m}\right)^2}} \Psi_{m,n}^2, \quad (49)$$

$$\phi_m = \tan^{-1} \frac{-2\varsigma\frac{\omega}{\omega_m}}{1-\frac{\omega^2}{\omega_m^2}}, \quad (50)$$

where $\Psi_{m,n}$ is the deflection mode shape at the node n and ς is the critical damping coefficient. The plate vibration effects between stiffeners can be considered by applying the corrected angular frequency ω_m, and generalised stiffness K_m according to Chapter 4.3.

To calculate the total response, including the effect of multiple vibration modes, modal superposition is required. Each mode needs to be divided into a complex format, i.e. X=X_{RE}+iX_{IM}, where X_{RE} is the real and iX_{IM} an imaginary part, which are found from the phase angle ϕ:

$$X_{RE,m,n} = X_{m,n}\cos\phi, \quad (51)$$

$$iX_{IM,m,n} = X_{m,n}\sin\phi. \quad (52)$$

The total response $X_{tot,n}$ and phase angle $\phi_{tot,n}$ at the frequency ω can be found by super-positioning the generalised modal responses of the real and imaginary parts:

$$X_{tot,n} = \sqrt{\left(\sum_{m=1}^{M} X_{RE,m,n}\right)^2 + \left(\sum_{m=1}^{M} iX_{IM,m,n}\right)^2}, \quad (53)$$

$$\phi_{TOT,n} = \tan^{-1} \frac{\sum_{m=1}^{M} iX_{IM,m,n}}{\sum_{m=1}^{M} X_{RE,m,n}}, \quad (54)$$

where M is the number of modes which are included in the forced vibration analysis.

In [P5] the equivalent element is utilised in forced vibration analysis of a cruise ship cabin deck structure - see Figure 17 - where it is excited by a 10-kN harmonic point force. The load position is shown in Figure 36. A uniform damping coefficient of 2% is used. The results obtained are additionally compared with an A-matrix model, in which only the membrane stiffness properties of the stiffened panel are considered. The results revealed that the utilisation of an A-matrix-type model for forced vibration analysis of the local structure leads to insufficient results; see Figure 35a. Additionally, increasing the mesh size will not improve the accuracy and lots of local unrealistic modes occur as the bending properties of the stiffened panel are not correctly considered, i.e. the bending stiffness is significantly lower than in reality. As [P5] shows, to calculate the forced response in the typical working range of the propellers, main engines, and thrusters of a cruise ship, bending and out-of-plane shear stiffness need to be considered and a minimum mesh size of two elements per web frame spacing should be used. Within this design range, the interaction with tertiary vibration modes is small and it is not necessary to apply correction. However, at higher frequencies than $\omega_{local}/3$, the interaction between the global modes becomes more active and the error of the ESL model starts to increase. To overcome this issue, the correction method that is presented needs to be applied and the model mesh size needs to be increased to four elements per web frame spacing; see[P5]. Very good correspondence with the fine mesh results can then be achieved until $\omega_{local}/1.5$. Despite the fact that the correction method presented in [P3] also allows the global vibration modes of the deck structure beyond that limit to be calculated, several local modes start to occur which are not covered by the theory presented in this thesis and because of that, the phase interaction between the modes is not calculated sufficiently; see Eq. 53. Figure 36 shows the response of the fine mesh model and ESL model at 20 Hz and 45 Hz. As can be seen, at a lower frequency the response shape that is obtained follows the fine mesh results very well. However, at 45 Hz, i.e. $\omega > \omega_{local}/1.5$, the shapes between the fine mesh and ESL model become different and other than clamped-clamped local modes start to dominate. However, in practical cruise ship design this limitation rarely becomes a question, as these response levels are usually less critical compared to the first vibration peaks; see Figure 35. General stiffness gets higher and much more energy is needed to create the undesired vibration levels.

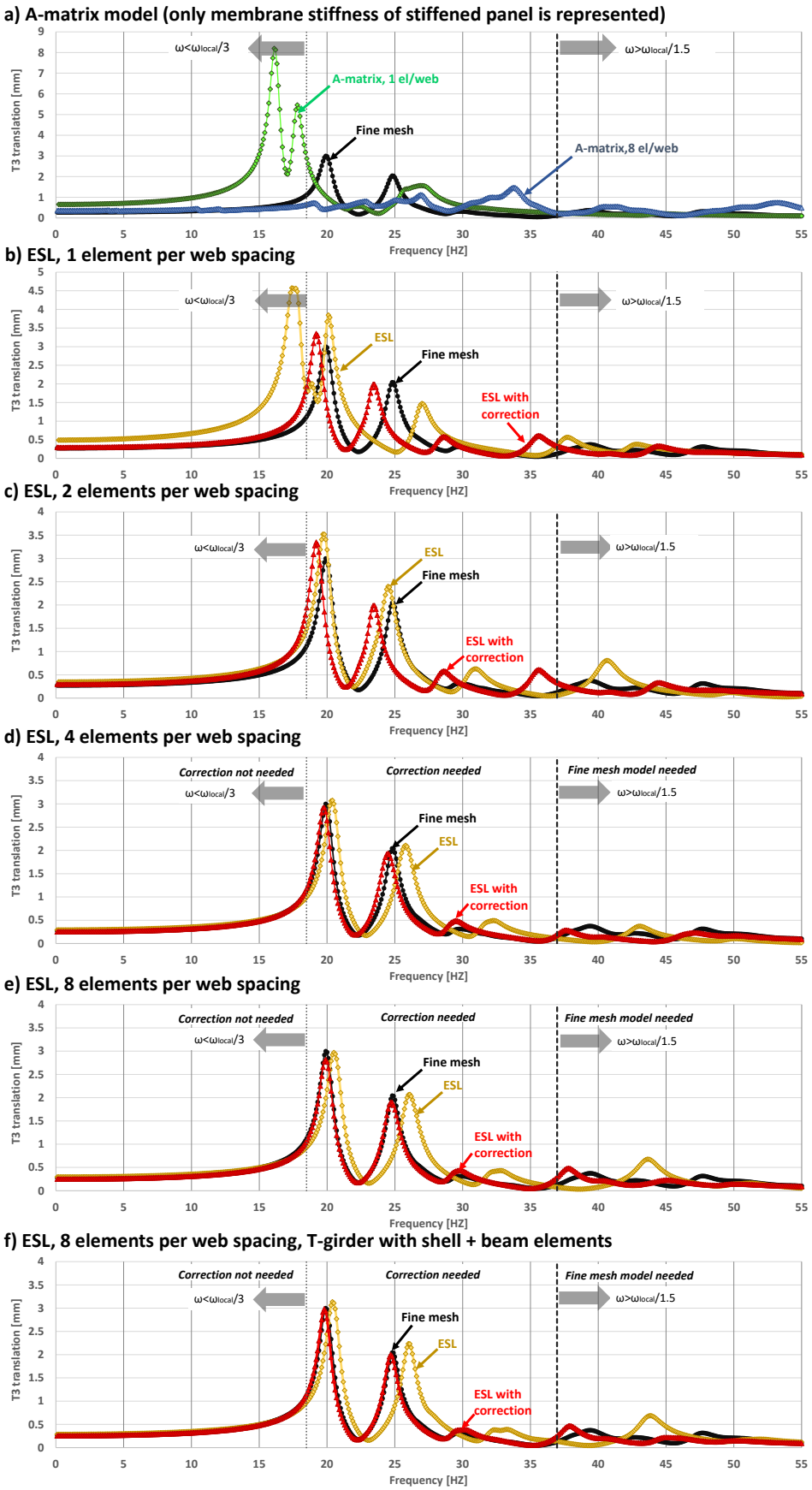

Figure 35. Forced vibration response of the cabin area under a 10-kN harmonic point force using (a) the A-matrix and (b-f) ESL theory-based models [P5].

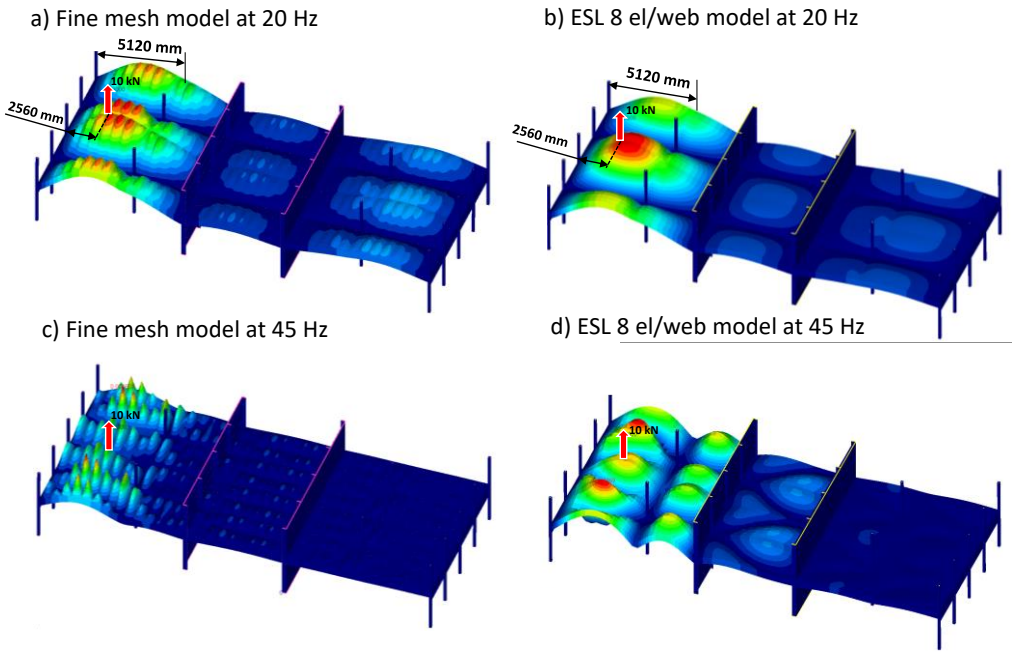

Figure 36. Response of the fine mesh and ESL theory-based models at 20 Hz and 45 Hz under a 10-kN harmonic point force [P5].

To illustrate the necessity of offset in local vibration analysis too, the results obtained are additionally compared with an ESL model where the offset is not done, and the reference plane corresponds to the geometrical mid-plane of the element; see Figure 37. As can be seen, it has a significant effect on the response. Not only are the frequencies of the vibration modes mismatched, but also the response amplitude becomes different.

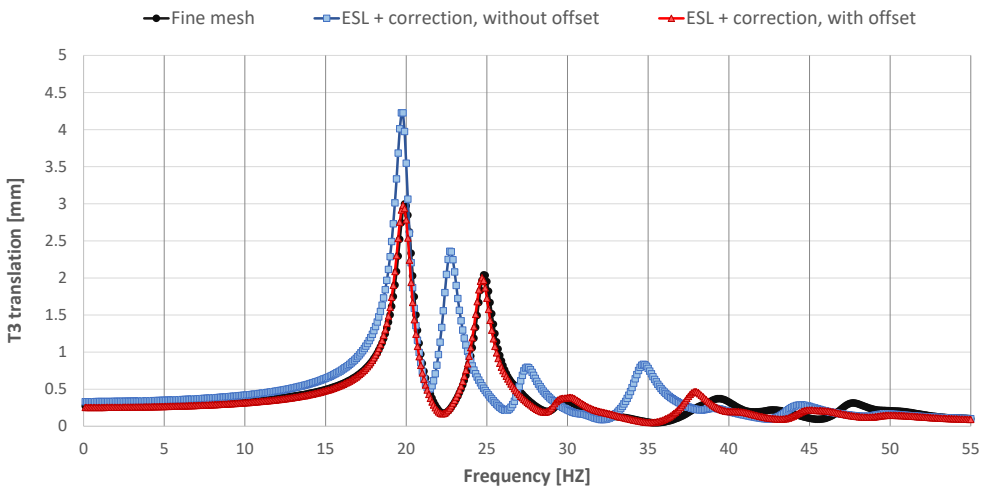

Figure 37. Forced vibration response of the cabin area for the corrected ESL model with and without the offset. The mesh size used is eight elements per webframe spacing.

5 Optimisation [P4]

As the previous chapters showed, the layer-wise ESL theory-based equivalent element that was developed brings the advantages of a fine mesh model with low computational cost. Compared to the commonly used A-matrix-type model, the amount of DOF remains equal when the same mesh density is used. These benefits are especially noticeable in the optimisation of a large ship structure, where thousands of design alternatives need to be created and analysed. In [P4] the equivalent element was utilised in modern passenger ship optimisation in the conceptual design phase. A new optimisation approach was developed which considers novel cruise ship design principles [19] and the peculiarities of a coarse mesh global FE model. The process is carried out using a user-defined MATLAB routine and the FE models are created and analysed using FEMAP with NX Nastran. In this research a population-based Particle Swarm Optimisation (PSO) algorithm is used, the concept of which was presented by Kennedy and Eberhart in [91] and later extended to structural engineering problems by Jalkanen in [92]. PSO has been found to be particularly computationally effective for large complex structures where thousands of design alternatives need to be analysed and several local minimum or maximum solutions can occur [93]. In [70] it was also applied for ESL theory when the optimisation of a web-core sandwich panel was performed. However, the equivalent element approach together with optimisation presented here is not limited to PSO and could also be applied for other genetic or evolution-based algorithms.

A flowchart of the optimisation process is presented in Figure 38. The first step is to create the global FE model and the next is to define the optimisation groups and their type. The groups can be divided into six categories; see Table 3. In the first three, the scantlings are changed during the optimisation, but all of the constraints, selected ones or none are evaluated. Most of the optimised groups belong to type 1, but in the conceptual design phase, there might be some structural members where not all the constraints are relevant, for example, T-girders or stiffener web buckling checks against tripping, as tripping brackets

will be added later in the basic or detail design phase. Types 4-6, on the other hand represent structural members where scantlings remain constant. For example T-girders under the deck are defined on the basis of outfitting and vibration requirements, but since they also receive hull girder bending loads, all (type 4) or part (type 5) of the constraints need to be evaluated. In addition, the global FE model might also include type 6 structures, which are modelled to some extent, but their actual design will be performed later, and thus optimisation and strength checks in the current stage are irrelevant [95]. A good example is the helideck or uppermost sundeck of the cruise ship. Because of this kind of type division, optimisation can already be performed in a very early design phase or only for part of the model. Next, the design variables of each group are defined. For a stiffened panel, the variables are material, plate thickness, stiffener type, and spacing, and as Eq. 7-8 and Eq. 18-19 show, they can be changed without remeshing the model by simply modifying the Young's and shear modulus, material density, and strength properties of the laminate element layers. The variables of the design space are constrained by production limits and the requirements of the classification society rules, which define the minimum plate thickness and beam properties; see e.g. [94]. The typical optimisation objectives are to reduce the hull mass, cost, and centre of gravity [5], [81], [93], [96].

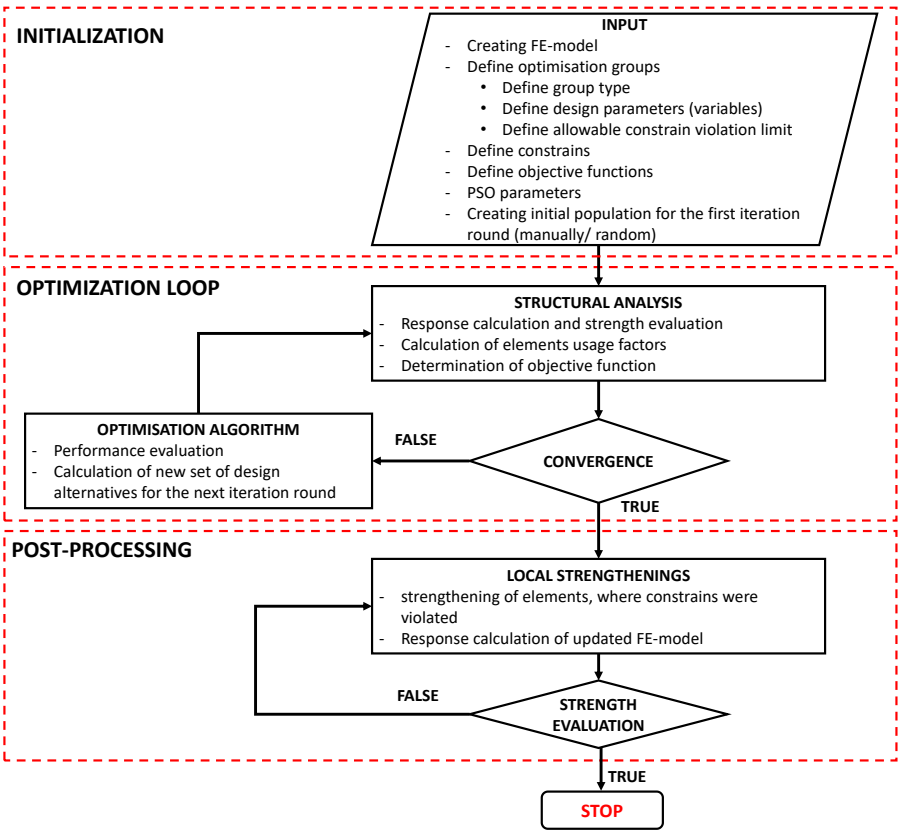

Figure 38: Flowchart of the optimisation process.

Table 3: Types of optimised groups used in [P4].

		Scantlings changed	
		Yes	No
Constraints evaluated	All	type 1	type 4
	Selected	type 2	type 5
	None	type 3	type 6

PSO starts with a predefined set of design alternatives, i.e. an initial population, which can be generated either manually or randomly. During the optimisation process it is updated every new generation by the previous position and velocity:

$$\boldsymbol{x}_{k+1}^{i} = \boldsymbol{x}_{k}^{i} + \boldsymbol{v}_{k+1}^{i}, \quad , \tag{55}$$

where $\boldsymbol{x}_{k}^{i}$ is the current position vector of the particle i and $\boldsymbol{v}_{k+1}^{i}$ is the velocity vector of the particle i in iteration round k. The velocity is found from following relationship:

$$\boldsymbol{v}_{k+1}^{i} = w\boldsymbol{v}_{k}^{i} + c_1 r_1\left(\boldsymbol{p}_{k}^{i} - \boldsymbol{x}_{k}^{i}\right) + c_2 r_2\left(\boldsymbol{p}_{k}^{g} - \boldsymbol{x}_{k}^{i}\right), \tag{56}$$

where $\boldsymbol{p}_{k}^{i}$ is the best location so far of the particle i and $\boldsymbol{p}_{k}^{g}$ is the best-known location of the entire swarm at a given iteration round k. The parameter w is inertia and the terms c_1 and c_2 are cognitive and social parameters. The terms r_1 and r_2 are uniformly distributed random numbers between 0 and 1. The purpose of the inertia term $w\boldsymbol{v}_{k}^{i}$ is to search a wider area of the design space, while the terms including $\boldsymbol{p}_{k}^{i}$ and $\boldsymbol{p}_{k}^{g}$ direct it towards a promising solution; see Figure 39. Constraints are considered by a penalty factor. Too small a penalty factor can lead to too many unsatisfying design alternatives, but one that is too large can leave out potentially good ones which violate the constraints only by a small amount. The optimisation loop continues until the required convergence in objective function or a predefined iteration number is achieved.

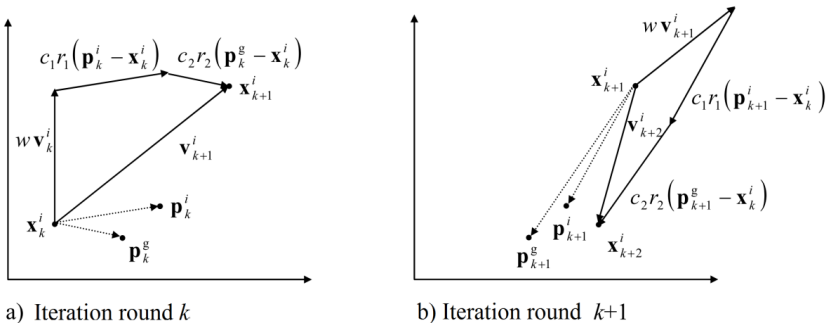

Figure 39: Iteration steps of PSO: a) iteration step from x_k^i to x_{k+1}^i b) iteration step from x_{k+1}^i to x_{k+2}^i [90].

When 3D FE models are used for response evaluation, singularity effects, structural discontinuities, and rapid changes of stiffness can cause locally highly stressed areas, i.e. stress concentrations. Additionally, in coarse mesh models, rounded corner openings are simplified into sharp corners, which provide sufficient stiffness [47], [48] but unrealistic stress peaks. The finer the mesh that is used, the higher these peak stresses will get. Despite their small contribution to the total area, they will dominate the optimisation groups and lead to a greater structural weight. In the shipbuilding process, these locations are treated separately in the basic and detail design phases by using local FE models with more precise geometry and applying locally thicker plates, stronger beams, or intermediate stiffeners. The same principle was applied in [P4], where a certain percentage of the optimisation group elements was allowed to violate the constraints. Thus, a design alternative is feasible if the ratio between the total area of infeasible and feasible elements of each group is less than a predefined value. This limit depends on the shipyard's production principles and can also be estimated on the basis of the experiences of a sister ship. Later, when an optimum result is achieved, these areas are strengthened separately by using common shipyard practices; see e.g. [97]. This constraint relaxation method is easy to apply, but a certain level of experience and expertise is required from the structural analyst to make such a judgement.

In a similar manner the vibration assessment is also executed later, after the optimum mid-frame scantlings are obtained. Including the forced vibration analysis of the ship already in the optimisation process is not economically and practically feasible. For each design alternative, hundreds of natural frequencies, together with the added fluid mass, need to be calculated. While quasi-static analysis can be performed in minutes, vibration analysis requires several hours. Additionally, the most critical vibration peaks are local and are treated individually by adding larger or additional beams or in some cases an extra pillar, rather than changing the general scantlings of the optimisation group. Therefore, despite the good performance of the ESL element in vibration analysis, the assessment is left out of the optimisation process.

The optimisation approach that was developed was applied to a generic prismatic cruise ship model; see Figure 12. As in Chapter 3.1, a quarter of a ship, together with symmetric boundary conditions, was used. The general mesh density was chosen to be two four-node (QUAD4) elements per web frame spacing, as this is found to be the optimal size for a global FE model of a large ship, considering the number of DOF versus accuracy [P1]. The same vertical

bending moments are used as in Chapter 3.1; they are generated by applying cosine shape pressure to the ship bottom elements; see Figure 11. On the basis of the authors' experience and the principles presented in [5], 16 optimisation groups were created; see Figure 10. All these groups belong to type 1; see Table 3. The rest of the structural members belong to type 4, i.e. the scantlings remain constant and strength evaluation will be performed. DNV-GL buckling and yielding constraints [98] were applied. The swarm size was chosen to be 20 and optimisation to last 75 iterations, leading to a total of 1500 design alternatives. The penalty factor for infeasible solutions was set to 1.5, the inertia term to 1.4, and the parameters c_1 and c_2 were chosen to be 2. Optimisation was performed for three separate cases by allowing a maximum constraint violation of 1%, 5% and 10% in each optimisation group for each load case. The objective of each case was to reduce the mass. Analysing the 1500 design alternatives – see Figure 40 – took a total of 50 hours using an HP Zbook 17" G2 Mobile Workstation (processor: Intel® Core™ i7-4940MX, memory: 32 GB RAM, storage: 512 GB SSD, graphics: Quadro K5100M).

Even though a simple prismatic model was used for the case study, the local highly stressed areas still have a significant influence on the objective function result; see Figure 40. Additionally, adding the required local strengthening will not noticeably influence the total steel mass of the ship; see Table 4. When a constraint violation of 5% was allowed, local strengthening then increased the mass by only 0.1% and in total a 6% lighter design was obtained compared to the 1% case. However, this effect is not linear and starts to decrease with higher percentages. For example, the step from 5 to 10% of constraint violation gave only 1.6% of additional benefit in the end result and the additional local strengthening already contributes 0.6% of the total mass. Therefore, at some point a higher constraint violation area is not justified because of the extra cost caused by adding local strengthening. The values that are presented illustrate a prismatic ship case and for actual cruise ship optimisation, the optimum constraint violation limit might be different. Figure 41 shows the X-normal stress in the deck plating of the final design of the 1% and 10% cases, which indicates that despite the mass changes, the load-carrying mechanism remains very similar between the cases. However, as [5] showed, it can change when additional objective functions are included.

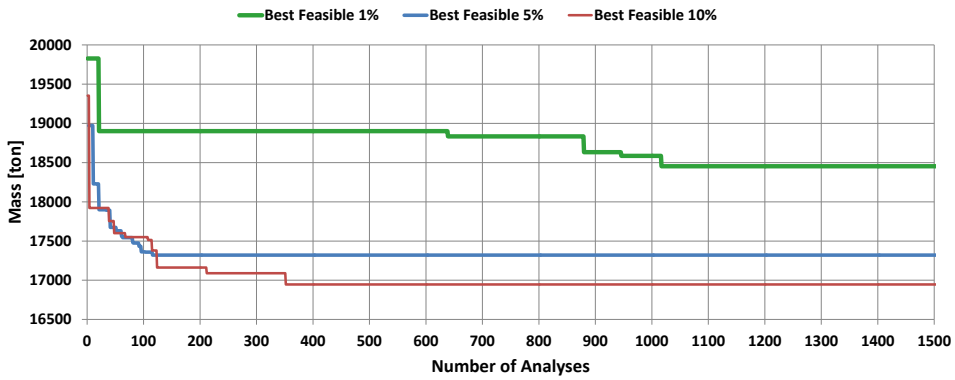

Figure 40: Convergence of objective function [P4].

Table 4: Total ship mass after optimisation and after local strengthening [P4].

	after optimisation		after adding local strengthening		
optimisation case	total mass [t]	difference between 1%	total mass [t]	mass increase [t]	difference from 1%
1 %	18454	100	18463	9	100
5 %	17321	93.9	17350	29	94.0
10 %	16946	91.8	17064	118	92.4

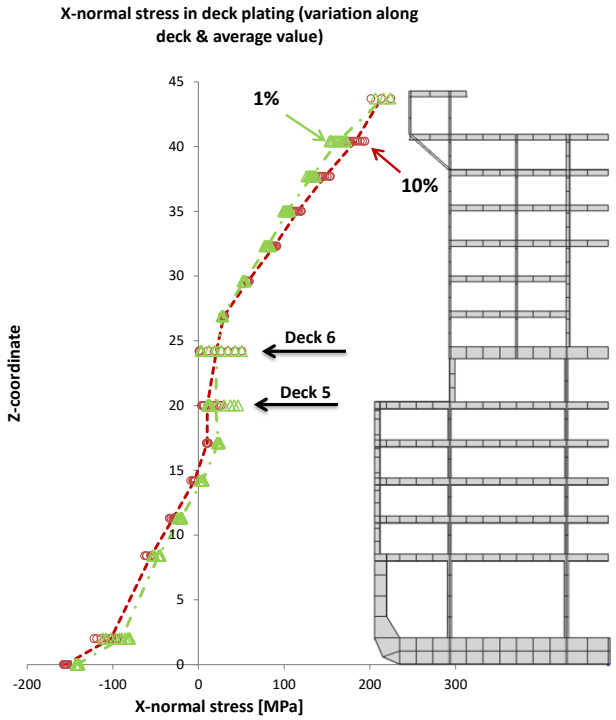

Figure 41: X-normal stress in deck plating (variation along deck as well as average value) for an optimised structure with local strengthening at L/2; two cases where 1 or 10% of constraint violation is allowed [P4].

6 Discussion & future work

This thesis presents an ESL theory-based equivalent element technique for stiffened panels to assess a ship's structural static and vibration response in the concept and basic design phases. Compared to other commonly used equivalent elements, e.g. [23], [49], [52], [53], [56], the element that was developed also enables local strength and vibration checks directly from a global FE model, making it possible to evaluate the feasibility of a concept much more accurately before the significant decisions are made.

The thesis research is divided into five papers and the main outcome of the work is summarised in Figure 42. When quasi-static analysis on the primary response level is performed, it is sufficient if only the membrane stiffness of a stiffened panel is presented: [11], [13], [16]. However, in practical design, it is still beneficial to already utilise the ESL theory-based laminate element for creating global a FE model. With the same mesh size, the DOF remains the same, but because of the layer-wise formulation, it is possible to obtain stresses in structural members separately and achieve lower post-processing time. As a result of the inclusion of bending and out-of-plane shear stiffness properties, the global FE model is suitable for calculating the secondary response against lateral pressures, where despite the homogenised representation of the stiffened panels, the plate bending response between the stiffeners can be considered by using the superposition principle, as in [66]. In a similar manner, it could be possible to consider deck plating stress changes resulting from the effective breadth effect under stiffener bending. The case studies also illustrate that it is crucial to have the element's reference in the right position to represent the stiffened panel membrane-bending couplings and interaction between the T-girders correctly; see [P1] and Figure 37.

With the layer-wise equivalent element presented here, the global FE model can be used for various types of elastic buckling and yielding strength analysis using analytical formulae [23] or classification rules [98]. As [P4] showed, utilising the ESL theory-based model in the conceptual design optimisation

process is beneficial, since the advantages of fine mesh can be obtained together with a coarse mesh (A-matrix) model's computational time. However, with a higher discretisation level, more local stress concentrations occur. These are typically caused by singularity effects or rapid changes in structural stiffness and can dominate the optimisation. In practice, these are treated later in the basic or detail design phases by local strengthening or higher-strength steel [97]. As [P4] showed, by allowing a certain percentage of the area to violate the optimisation constraints and later strengthening these areas locally, it is possible to obtain significantly lighter design. The equivalent element was applied for a PSO algorithm-based optimisation process, but it can easily be utilised in any other FE model-based ship optimisation approach, e.g. in [96]. In this thesis, optimisations were performed for quasi-static load cases. Including vibration seems possible, but it will make the whole optimisation process extremely time-consuming. For example, propellers- and main engines-induced forced vibration analysis requires 100-200 times more calculation time than hull girder bending response analysis. In addition, typically, the problematic areas are local and the structural improvements are made after the general scantlings of the hull girder are defined.

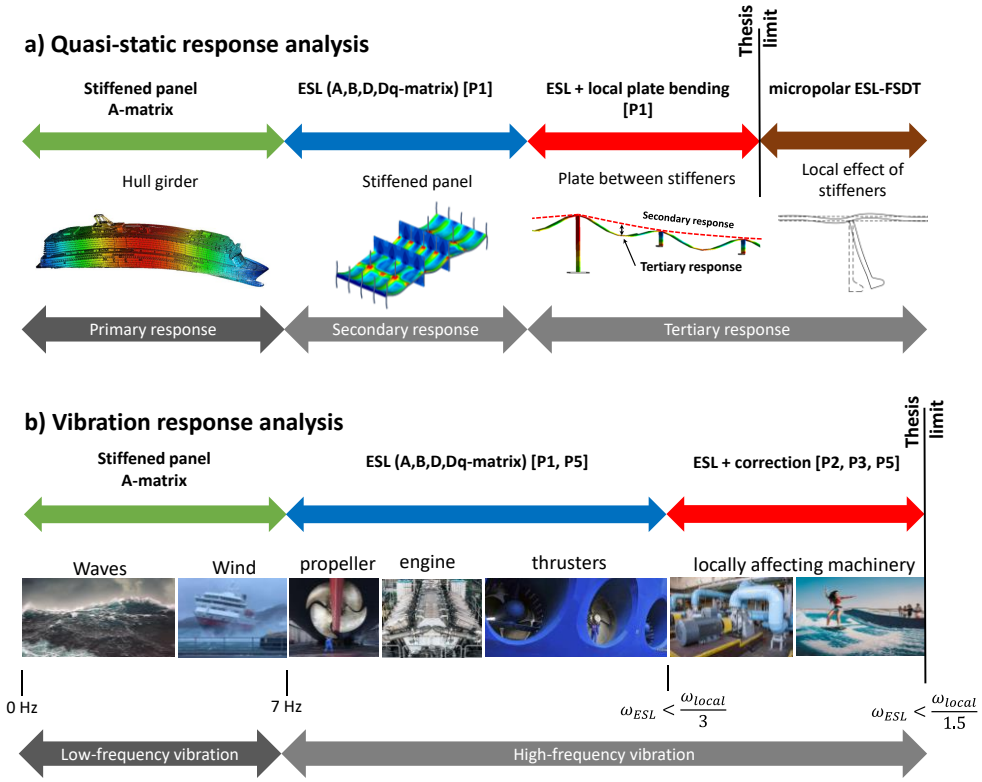

Figure 42: Scope of thesis and validity range of A-matrix and ESL theory-based FE model.

[P5] showed that when a global ship FE model is used for global vibration analysis, it is sufficient to consider only the membrane stiffness of the stiffened

panel. For propellers-, engines-, and thrusters -induced vibration response analysis, this modelling technique is inaccurate and bending and out-of-plate shear properties of the stiffened panels should be included. By using the ESL theory-based equivalent element, an accurate response can be achieved until the frequencies being investigated are three times smaller than the local plate frequencies between the stiffeners, i.e. $\omega<\omega_{local}/3$ [P5]. Beyond that, a correction method which considers the plate vibration effects between the stiffeners needs to be applied. When the aim is to calculate only the natural frequencies of stiffened panels for half-wave modes, then a simple single-degree-of-freedom spring-mass system-based method can be used [P2]. For deck structures where girders and bulkheads are also included, this method is limited and a more advanced kinetic and strain energy-based correction method, presented in [P3], can be applied. [P5] showed that this correction method is also suitable for forced vibration analysis where the response curve needs to be adjusted in two directions. The corrected natural frequency will move the curve into the correct position along the horizontal axis and the updated general mass and stiffness will perform the adjustment in a vertical direction; see Figure 35. With this correction, the range of validity of the equivalent element can be extended from $\omega<\omega_{local}/3$ to $\omega<\omega_{local}/1.5$. After this limit the natural frequencies that are obtained can still be corrected [P3], but as several local modes cannot be found and described with ESL, super-positioning and phase interaction in forced vibration analysis for such frequencies are performed in an inadequate way. Nevertheless, the achievements of this thesis are significant in relation to the decoupled models for vibrations, as shown by [99], [100], [101].

During the case studies, several mesh sensitivity analyses were performed, and the findings are summarised in Table 5. Although for investigating the primary response a mesh density of one element per web frame spacing is sufficient, the optimal mesh size for creating a global FE model seems to be two elements per web frame spacing. Then relevantly good accuracy in local vibration analysis can also be obtained. However, this size is valid for a lumped mass matrix, where as a result of coarse mass distribution an error cancelling effect occurs. When a consistent mass matrix in which the mass distribution is expressed by shape functions is used instead, this cancelling effect disappears and a mesh size of two elements per web frame spacing can lead to too stiff a structure [102]. If the response under lateral loads needs to be investigated, the mesh should be refined to four elements per web frame spacing. This mesh size also seems optimal for modelling shell and bulkhead openings [48]. Therefore, for special vessels, a finer mesh size for the global FE model seems justified.

Table 5: Recommended minimum mesh size for ESL theory-based model when a four-node shell element is used.

Analysis type	Primary level	Secondary level	Tertiary level
Quasi-static	1 el/web	4 el/web	4 el/web
Vibration (lumped mass matrix)	1 el/web	2 el/web	4 el/web

The equivalent element presented here is limited to linear-elastic analysis. As new cruise ship concepts become more complex and lightweight-oriented, extending the global FE model beyond that limit is an attractive topic to study. The ESL theory-based global FE model can be used in combination with the Idealised Structural Unit Method (ISUM), in a similar way to how it was done for A-matrix elements in [103]. Additionally, the extension of the equivalent element theory itself for geometrical and material non-linearity seems possible. Compared to orthotropic plate methods, e.g. [52], [53], membrane-bending coupling and out-of-plane shear stiffness are included. Furthermore, the stresses in different structural members, i.e. plates, webs and flanges, can be analysed separately. As a result, higher accuracy the ultimate strength analysis of stiffened panels could be achieved. The previous research on web-core sandwich panels, e.g. [74], [75], [76], reveals that when linear stiffness matrices are used, ESL can capture the panel buckling with very good accuracy until the point where local plate buckling between webs occurs. To overcome this issue the stiffness properties need to be modified in increments as the load increases and local buckling occurs, similarly to [53], [104], [105], [106]. In [107] ESL-FSDT was utilised in the ultimate strength analysis of a stiffened panel and grillage structure, where non-linear ABD matrices were applied together with geometrical imperfections. The UGENS subroutine in Abaqus, in which geometrical and material non-linear properties are predefined using a unit cell approach, was used. As a result, the ESL theory-based element behaves differently under tension and compression and for each load increment the subroutine modifies the ESL stiffness properties - see Eq. 13 - of each shell element separately on the basis of its strain state. For more details, see [108]. Very good correspondence with a 3D fine mesh until post-ultimate response was observed. The extension beyond that limit and for the entire ship structure needs to be studied further. Non-linear analysis of the ESL theory-based element can alternatively be performed by applying advanced micropolar ESL-

FSDT theory, as was done for sandwich panels in [77] and [78]. In both methods extension and validation to a global-scale ship problem need to be performed.

The various case studies presented in this thesis are cruise ship-oriented, but the equivalent element introduced here could also be utilised for other ship types such as container and RoRo ships, bulkers, and tankers. It would be especially attractive to implement it in the vibration analysis of cargo ship superstructures, as crew and structural fatigue caused by unpredicted high vibration levels is a common problem [109], [110]. This is due to the fact that crew accommodation and working spaces are located in a relatively flexible tower-like structure, directly under a powerful low-speed engines and propeller. These types of case studies are left for future work.

7 Conclusions

The aim of this doctoral thesis was to develop an equivalent element technique for representing stiffened panels to assess a ship's global and local static and vibration response with high accuracy and low computational cost. On the basis of the research, the following conclusions can be drawn:

- Despite the fact that a ship's stiffened panels do not represent the classical periodic continuum mechanics structure, where the ratio between micro and macro scale should be infinitely small, i.e. S/B →0, applying a homogenisation method still seems justified. Actual 3D structure behaviour can be represented with very low computational cost and relatively high accuracy.
- The stiffened panel can be represented using a three-layer laminate element which follows ESL-FSDT. The homogenised properties of the layers can be found from the Rule of Mixtures. As a result of the layer-wise formulation, the response can be evaluated in the plate, stiffener web, and flange separately. The laminate element reference plane should be defined in a way that allows geometrically exact coupling between the surrounding structures.
- As a result of homogenisation the plate bending effect between stiffeners is neglected and in some cases needs to be reconsidered. In static response analysis this can achieved by simply applying the super-positioning principle. For free and forced vibration the homogenisation is justified when the frequencies being investigated are 2.5-3 times smaller than the local plate frequencies between the stiffeners. This covers a typical range of ship propellers-, main engines- and thrusters-induced vibration. Beyond that limit two correction methods are developed. For calculating the natural frequencies of a stiffened panel, a single-degree-of-freedom spring-mass system-based solution can be used. For free and forced vibration analysis of more complex structures, a kinetic and strain energy-based method is available.

- Compared to the existing commonly used equivalent elements, which are based on membrane or bending actions alone, significantly higher accuracy can be achieved, while the computational cost remains very low. A mesh size of one four-node element per web frame spacing is required for the hull girder level. For local vibration and static response analysis, the FE model should have at least two and four elements between the web frames, respectively.
- The high accuracy of the laminate element, together with low modelling and computational cost and layer-wise formulation, makes it convenient for utilisation in the optimisation of large complex structures. In addition to hull girder loads, local lateral loads can also be directly applied to the global FE model.
- The equivalent element presented here is limited to linear-elastic analysis. However, the extension of equivalent element theory itself for geometrical and material non-linearity seems possible and could provide remarkable computational savings for analysing large complex structures.

References

[1] Bergström M. Longitudinal Strength Analysis of a Cruise Ship with a Narrow Superstructure, Master's Thesis, Aalto University, 2010.

[2] Tsitsilonis K, Stefanidis F, Mavrelos C, Gad A, Timmerman M, Vassalos D, Kaklis P. Concept design considerations for the next generation of mega-ships. Marine Design XIII: Proceedings of the 13th International Marine Design Conference (IMDC 2018), 2018;1:579-588.

[3] Parmasto O, Romanoff J, Remes H. Hull-Superstructure Interaction Induced Secondary Effects in Passenger Ships. Proceedings of the 12th International Symposium on Practical Design of Ships and Other Floating Structures (PRADS2013), 2013:290-294.

[4] Lillemäe I, Remes H, Romanoff J. Influence of initial distortion of 3 mm thin superstructure decks on hull girder response for fatigue assessment. Marine Structures 2014;37:203-218.

[5] Romanoff J, Remes H, Varsta P, Naar H, Niemelä A, Jelovica J, Klanac A, Bralic S. Hull-superstructure interaction in optimized passenger ships, Ships and offshore structures, 2013;8:612-620.

[6] Heiskari J. On the design criteria of large insulating glass structures in cruise ships. Master's Thesis, Aalto University, 2020.

[7] Evegren F, Hertzberg T, Rahm M. LASS-C; Lightweight construction of a cruise vessel, SP Report 2011:12, ISBN 978-91-86622-43-5; 2011.

[8] DNV-GL, Pt. 6 Ch. 8, Living and working conditions; October 2015.

[9] Evans J. Basic Design Concepts. Naval Engineers Journal, 1959;71(4):671-678.

[10] DNV-GL, Pt. 3 Ch. 3, Structural design principles; January 2017.

[11] Wang ED, Bone JS, Ma M, Dinovitzer A. Guidelines for evaluation of marine finite element analyses, SSC-475; December 2019.

[12] Gudmunsen MJ. The Structural Design of Large Passenger Ships, Lloyds Register of Shipping; September 2000.

[13] DNV-GL, Finite Element Analysis; October 2015.

[14] Bureau Veritas (BV), Rules for the Classification of Ships, Part F: Additional Class Notations, January 2020.

[15] American Bureau of Shipping, Guidance notes on ship vibration; 2018.

[16] Norwood MN, Dow RS, Dynamic analysis of ship structure, Ship and Offshore Structures 2013;8(3-4):270-288.

[17] Iijima K, Yao T, Moan T. Structural response of a ship in severe seas considering global hydroelastic vibrations, Marine Structures 2008;21(4):420-445.

[18] Senjanovic I, Vladimir N, Tomic M, Hadžić N. An integral procedure for ship vibration analysis. Proceedings of the 22nd SORTA Symposium, 2016;257-269.

[19] Keiramo M. Pathways of the Creative Journey - the Significance of a Cruise Ship Concept Design, Doctoral Thesis, Aalto University, 2021.

[20] Xu M, Garbatov Y, Guedes Soares C. Ultimate strength assessment of a tanker hull based on experimentally developed master curves. Journal of Marine Science and Application 2013;12:127–139.

[21] Gordo J, Guedes Soares C. Interaction Equation for the Collapse of Tankers and Containerships Under Combined Bending Moments. Journal of Ship Research 1997;41(3):230-240.

[22] Paik J. A Guide for the Ultimate Longitudinal Strength Assessment of Ships. Marine Technology 2004;41(3)122-139.

[23] Hughes OF. Ship structural design. Jersey city, New Jersey: Society of Naval Architects and Marine Engineers; 1988.

[24] Vasta J. Lessons learned from full-scale ship structural tests. SNAME Trans. 1958;66:165-243.

[25] Fransman JW. The influence of passenger ship superstructures on the response of the hull girder. RINA Trans. 1988;131:57–71.

[26] Crawford L. Theory of long ship's superstructures. Trans. Soc. Nav. Archit. 1950;58:693-699.

[27] Bleich HH. Nonlinear distribution of bending stresses due to distortion of cross section. J. Applied Mechanics 1952;20:95.

[28] Terazava K, Yagi J. The effect of superstructure on the strength of ship (Report No. 2). Journal of the Society of Naval Architects of Japan 1957;101:183-191.

[29] Terazava K, Yagi J. The effect of superstructure on the strength of ship (Report No. 4). Journal of the Society of Naval Architects of Japan 1958;103:165-172.

[30] Fransman J. The influence of passenger ship superstructures on the response of the hull girder. Trans. RINA 1988.

[31] Naar H, Varsta P, Kujala P. A theory of coupled beams for strength assessment of passenger ships. Marine Structures 2004;17:590-611.

[32] Niemeläinen M. Computional Method for Evaluation of Hull Girder Strength in Concept Design State. Master's Thesis. Helsinki University of Technology, 2007.

[33] Klanac A, Ehlers S, Jelovica J. Optimization of crashworthy marine structures. Marine Structures 2009;22:670-690.

[34] Moan T, Berge S. ISSC 1997: Proceedings of the 13th International Ship and Offshore Structure Congress, Pergamon 1998.

[35] Paulling JR, Payer HG. Hull-Deckhouse Interaction by Finite Element Calculations, Annual Meeting of Society of Naval Architects and Marine Engineers, November 13-16, 1968:281-307.

[36] Spence JH, Favini EA, Page CA. SSC-470 Finite element modeling methods: vibration analysis for ships, 2015.

[37] Prebeg P, Zanic V, Vazic B. Application of a surrogate modeling to the ship structural design. Ocean Engineering 2014;84:259-272.

[38] Zanic V, Andric J, Prebeg P. Design synthesis of complex ship structures. Ships and Offshore Structures 2013;8:383-403.

[39] Sun L, Wang D. A new rational-based optimal design strategy of ship structure based on multi-level analysis and super-element modelling method. Journal of Marine Science Applications 2011;10:272-280.

[40] Boote D, Pais T, Dellepiane S. Vibration of superyacht structures: comfort rules and predictive calculations. In: Proceedings of the 4th International Conference on Marine Structures (MARSTRUCT2013), 2013:37-44.

[41] Macchiavello S, Tonelli A. Pleasure vessel vibration and noise finite element analysis, 6th BETA CAE Internatational Conference, 2015.

[42] Pais T, Analytical and numerical computation of added mass in vibration analysis for a superyacht, Ships and Offshore Structures 2018;13(4):443-450.

[43] Lin TR, Pan P, O'Shea PJ, Mechefske CK. A study of vibration and vibration control of ship structures. Marine Structures 2009;22(4):730-743.

[44] Moro L, Biot M, Brocco E, Lorenzo FD, Vassallo P. Hull vibration analysis of river boats, International Conference IDS2013 – Amazonia, 2013.

[45] Andric J, Zanic V. The global structural response model for multi-deck ships in concept design phase, Ocean Engineering 2010;37:688-704.

[46] Heder M, Ulfvarson A. Hull beam behaviour of passenger ships. Marine Structures 1991;4(1): 17–34.

[47] Fricke W, Gerlach B. Effect of Window Openings on the Stiffness of Walls and Bulkheads in ships, Ships and Offshore Structures 2015;10(3):256-271.

[48] Kaldoja M. Modeling of Ship's Side Shell Openings in Global Finite Element Models. Master's Thesis, Aalto University, 2017.

[49] Davies JD. A Finite Element to Model the In-Place Response of Ribbed Rectangular Panels, Master's Thesis, School of Mechanical and Industrial Engineering, University of New South Wales, 1976.

[50] Hughes OF, Mistree F, Zanic V. A Practical Method for the Rational Design of Ship Structures. Journal of Ship Research 1980;24(2):101-113.

[51] Mobasher Amini A, Dureisseix D, Cartraud P, Buannic N. A domain decomposition method for problems with structural heterogeneities on the interface: Application to a passenger ship, Computer Methods in Applied Mechanics and Engineering 2009;198(41-44):3452-3463

[52] Paik JK, Thayamballi AK, Ju Kim B. Large deflection orthotropic plate approach to develop ultimate strength formulations for stiffened panels under combined biaxial compression/tension and lateral pressure. Thin-Walled Structure 2001;39:215–46.

[53] Benson S, Downes J, Dow RS. Overall buckling of lightweight stiffened panels using an adapted orthotropic plate method, Engineering Structures 2015;85;107-117.

[54] Allman DJ. A compatible triangular element including vertex rotations for plane elasticity analysis. Computers and Structures 1984;19(1/2):1-8.

[55] Katili I. A new discrete Kirchhoff-Mindlin element based on Mindlin-Reissner plate theory and assumed shear strain fields-part I: an extended DKT element for thick-plate bending analysis. Int J Numerical Methods in Engineering 1993;36(11):1885-1908.

[56] Satish Kumar YV, Mukhopadhyay M. Finite element analysis of ship structures using a new stiffened plate element, Applied ocean Research 2000;22:361-374.

[57] Coenen EWC, Kouznetsova VG, Geers MGD. Computational homogenization for heterogeneous thin sheets. International Journal for Numerical Methods in Engineering 2010;83:1180-1205.

[58] Kouznetsova VG, Geers MGD, Brekelmans WAM, Multi-scale second-order computational homogenization of multi-phase materials: a nested finite element solution strategy, Computer Methods in Applied Mechanics and Engineering 2004;193(48–51):5525-5550.

[59] Cartraud P, Messager T, Computational homogenization of periodic beam-like structures, International Journal of Solids and Structures 2006;43(3–4):686-696.

[60] Geers MGD, Kouznetsova VG, Brekelmans WAM, Multi-scale computational homogenization: Trends and challenges, Journal of Computational and Applied Mathematics 2010;234(7):2175-2182.

[61] Miehe C, Schröder J, Becker M. Computational Homogenization Analysis in Finite Elasticity: Material and Structural Instabilities on the Micro- and Macro-Scales of Periodic Composites and their Interaction. Computer Methods in Applied Mechanics and Engineering 2002 191(44):4971-5005.

[62] Reddy JN. Mechanics of laminated composite plates and shells – theory and analysis, 2nd ed. CRC Press, 2004.

[63] Carrera E. Historical review of Zig-Zag theories for multilayered plates and shells, Applied Mechanics Reviews 2003;56(3):287–308.

[64] Buannic N, Cartraud P, Quesnel T. Homogenization of corrugated core sandwich panels, Composite Structures 2003; 59(3): 299-312.

[65] Lewinski T, Telega JJ. Plates, laminates and shells. Asymptotic analysis and homogenization. Singapore: World Scientific; 1999.

[66] Romanoff J, Varsta P. Bending response of web-core sandwich plates. Composite Structures 2007;81:292-302.

[67] Voigt W. Ueber die Beziehung zwischen den beiden Elasticitätsconstanten isotroper Körper. Annalen der Physik 1889;274: 573–587.

[68] Reuss A. Berechnung der Fließgrenze von Mischkristallen auf Grund der Plastizitätsbedingung für Einkristalle. Zeitschrift für Angewandte Mathematik und Mechanik 1929;9:49–58.

[69] Romanoff J, Klanac A. Design optimization of steel sandwich hoistable car decks applying homogenized plate theory. Journal of ship production 2008;24(2):108-115.

[70] Romanoff J. Optimization of web-core steel sandwich decks at concept design stage using envelope surface for stress assessment. Engineering structures 2014;66:1-9.

[71] Avi E, Lillemäe I, Romanoff J, Niemelä A. Equivalent shell element for ship structural design. Ship and Offshore Structures 2015;20(3):239-255.

[72] Reinaldo Goncalves B, Jelovica J, Romanoff J. A homogenization method for geometric nonlinear analysis of sandwich structures with initial imperfections. Int J Solids Struct 2016;87(1):194– 205.

[73] Romanoff J, Interaction between laser-welded web-core sandwich plate and girder under bending loads, Thin-Walled Structures 2011;49:772-781.

[74] Jelovica J, Romanoff J. Buckling of sandwich panels with transversely flexible core: correction of the equivalent single-layer model using thick-faces effect. Journal of Sandwich Structures & Materials 2020;22(5):1612-1634.

[75] Jelovica J, Romanoff J, Ehlers S, Varsta P. Infuence of weld stiffness on buckling strength of laser-welded web-core sandwich plates, Journal of Constructional Steel Research 2012;77:12-18.

[76] Jelovica J, Romanoff J. Load-carrying behaviour of web-core sandwich plates in compression, Thin-Walled Structures 2013;73:264-272.

[77] Karttunen AT, Reddy JN, Romanoff J. Two-scale micropolar plate model for web-core sandwich panels International Journal of Solids and Structures 2019;170:82–94.

[78] Nampally P, Karttunen AT, Reddy JN Nonlinear finite element analysis of lattice core sandwich plates. International Journal of Non-Linear Mechanics, 2020 (accepted manuscript)

[79] Tilander J, Patey M, Hirdaris S. Springing Analysis of a Passenger Ship in Waves. Journal of Marine Science and Engineering 2020;8(7):492.

[80] Schellin TE, Perez de Luas A, Longitudinal strength of a high-speed ferry, Applied Ocean Research 2004;26:298-308.

[81] Rigo P. Least-cost structural optimization oriented preliminary design. Journal of ship production 2001;17(4):202-215.

[82] Ilus M. Matkustajalaivan rungon rakentamiskustannukset ja niiden alentamiskeinot. Master'sthesis, Helsinki University of Technology, 1999.

[83] Hill R. Elastic properties of reinforced solids: some theoretical principles. Journal of the Mechanics and Physics of Solids 1963; 11:357–372

[84] Aboudi J, Steven M, Arnold SM, Bednarcyk B. Micromechanics of composite materials - a generalised multiscale analysis approach, Elsevier, 2013.

[85] FEMAP User Guide, Version 2020.2.

[86] Det Norske Veritas, Pt.3 Ch.1 Hull structural design - ships with length 100 meters and above; July 2014.

[87] Naar H. Ultimate Strength of Hull Girder for Passenger Ships, Doctoral Thesis, Aalto University, 2006.

[88] Weaver W, Timoshenko S, Young D. Vibration problems in engineering. John Wiley & Sons; 1990.

[89] Blevins RD. Formulas for Natural Frequency and Mode Shape, Krieger Publishing Company, Malabar, Florida; 1995.

[90] Rao SS, Vibration of Continuous Systems, John Wiley & Sons Inc, 2007. ISBN-13 978-0-471-77171-5

[91] Kennedy J, Eberhart R. 1995. Particle swarm optimization. IEEE Conf. of neural networks, Piscataway, pp. 1942-1948

[92] Jalkanen J. Palvelualgoritmi kantavien rakenteiden optimoinnissa. Rakenteiden Mekaniikka 2006;39(2):23-35.

[93] Ma M, Hughes O, McNatt T. Ultimate Limit State Based Ship Structural Design Using Multi-Objective Discrete Particle Swarm Optimization, Proceedings of the ASME 2015 34th International Conference on Ocean,Offshore and Arctic Engineering, OMAE2015, Volume 3: Structures, Safety and Reliability, 2015.

[94] DNV-GL, Pt. 3 Ch. 1, General principles; July 2016.

[95] Rigo P, Ehlers S, Andrić J. Design of Innovative Ship Concepts Using an Integrated Decision Support System for Ship Production and Operation. Brodogradnja 2010;61(4):367-381.

[96] Andrić J, Prebeg P, Zanic V. Multi-level Pareto supported design methodology-application to RO-PAX structural design. Marine Structures. 2019;67:102638.

[97] Lillemäe-Avi I, Liinalampi S, Lehtimäki E, Remes H, Lehto P, Romanoff J, Sören E, Niemelä A. Fatigue strength of high-strength steel after shipyard production process of plasma cutting, grinding, and sandblasting. Welding in the World 2018;62:1273–1284.

[98] DNV-GL, Pt.3 Ch.8, Buckling; July 2020.

[99] Lok TS, Cheng QH. Free vibration of clamped orthotropic sandwich panel, Journal of Sound and Vibration 2000;229(2):311-327.

[100] Lok TS, Cheng QH. Free and forced vibration of simply supported, of orthotropic sandwich panel, Computers and Structures 2001;79(3)301-312.

[101] Lok TS, Cheng QH. Bending and forced vibration response of clamped orthotropic thick plate and sandwich panel, Journal of Sound and Vibration 2001;245(1):63-78.

[102] Avi E. Equivalent shell element for ship structural design, Master's Thesis, Aalto University, 2011.

[103] Pei Z, Iijima K, Fujikubo M, Tanaka S, Okazawa S, Yao T. Simulation on progressive collapse behaviour of whole ship model under extreme waves using idealized structural unit method. Marine Structures 2015;40:104-133.

[104] Byklum E, Steen E, Amdahl J. A semi-analytical model for global buckling and postbuckling analysis of stiffened panels, Thin-Walled Structures 2004;42(5):701-717.

[105] Byklum E, Amdahl J. A simplified method for elastic large deformation analysis of plates and stiffened panels due to local buckling, Thin-Walled Structures 2002;40(11):925-953.

[106] Steen E, Byklum E, Hellesland J. Elastic postbuckling stiffness of biaxially compressed rectangular plates. Engineering Structures 2008;30(10):2631-2643.

[107] Putranto T, Kõrgesaar M, Jelovica J, Tabri K, Naar H. Ultimate strength assessment of stiffened panel under uni-axial compression with non-linear equivalent single layer approach, Marine Structures 2021;78:103004

[108] Goncalves BR, Jelovica J, Romanoff J. Abaqus UGENS subroutine for nonlinear analysis of periodic panels. 2016 http://urn.fi/URN:ISBN:978-952-60-6905-0

[109] Lloyd's Register, Guidance Notes: General overview of ship structural vibration problems, September 2015.

[110] Godaliyadde D, Phylip-Jones G, Yang ZL, Batako AD, Wang J. An Analysis of Ship Hull Vibration Failure Data, Safety and Reliability. 2009; 29(1):15-26.

Predicting the strength and vibration response of a large passenger ship is a challenging task with several contributing factors. The calculation methods need to be computationally light to enable design optimization, but still accurate enough to describe both global and local behaviour in a way that the design constraints are properly assessed. The common approach is to use the finite element method, where the entire ship is described with very coarse mesh and the stiffeners together with plating are modelled using equivalent, homogenized, elements. The objective of this thesis is to introduce a more advanced equivalent element that allows increased accuracy of the coarse mesh global finite element model, allowing assessment of challenging ship concepts with lower risk and cost.

Aalto-DD 133/2021

ISBN 978-952-64-0531-5 (printed)
ISBN 978-952-64-0532-2 (pdf)
ISSN 1799-4934 (printed)
ISSN 1799-4942 (pdf)

Aalto University
School of Engineering
Department of Mechanical Engineering
www.aalto.fi

BUSINESS + ECONOMY

ART + DESIGN + ARCHITECTURE

SCIENCE + TECHNOLOGY

CROSSOVER

DOCTORAL DISSERTATIONS